Journal of Medicinal Chemistry

Article

Synthesis of 5-Nitro-2-furancarbohydrazides and Their *cis*-Diamminedichloroplatinum Complexes as Bitopic and Irreversible Human Thioredoxin Reductase Inhibitors

Rgis Millet, Sabine Urig, Judit Jacob, Eberhard Amtmann, Jacques-Philippe Moulinoux, Stephan Gromer, Katja Becker, and Elisabeth Davioud-Charvet

J. Med. Chem., **2005**, 48 (22), 7024-7039• DOI: 10.1021/jm050256l • Publication Date (Web): 07 October 2005

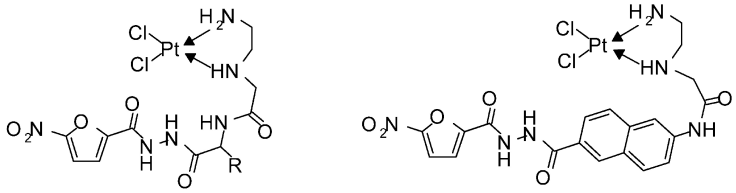

R = phenyl, 2-naphthylmethyl, 1-naphthylmethyl

More About This Article

Additional resources and features associated with this article are available within the HTML version:

- Supporting Information
- Access to high resolution figures
- Links to articles and content related to this article
- Copyright permission to reproduce figures and/or text from this article

View the Full Text HTML

Journal of Medicinal Chemistry is published by the American Chemical Society. 1155 Sixteenth Street N.W., Washington, DC 20036

Synthesis of 5-Nitro-2-furancarbohydrazides and Their *cis*-Diamminedichloroplatinum Complexes as Bitopic and Irreversible Human Thioredoxin Reductase Inhibitors

Régis Millet,[†,⊥,⊗] Sabine Urig,[#,⊥] Judit Jacob,[§] Eberhard Amtmann,[||] Jacques-Philippe Moulinoux,[‡] Stephan Gromer,[§] Katja Becker,[#] and Elisabeth Davioud-Charvet[†,§,*]

UMR 8525 CNRS-Université Lille II-Institut Pasteur de Lille, Institut de Biologie de Lille, 1 rue du Professor Calmette, BP447 59021 Lille Cedex, France, Interdisciplinary Research Center, Giessen University, Heinrich Buff-Ring 26-32, D-35392 Giessen, Germany, Department D060, German Cancer Research Centre, Im Neuenheimer Feld 280, D-69120 Heidelberg, Germany, Groupe de Recherche en Thérapeutique Anticancéreuse, Université Rennes I, 2 Av du Professeur Léon Bernard, 35043 Rennes Cedex, France, and Biochemie-Zentrum der Universität Heidelberg, Im Neuenheimer Feld 504, D-69120 Heidelberg, Germany

Received March 21, 2005

The human selenoprotein thioredoxin reductase is involved in antioxidant defense and DNA synthesis. As increased thioredoxin reductase levels are associated with drug sensitivity to cisplatin and drug resistance in tumor cells, this enzyme represents a promising target for the development of cytostatic agents. To optimize the potential of the widely used cisplatin to inhibit the human thioredoxin reductase and therefore to overcome cisplatin resistance, we developed and synthesized four *cis*-diamminedichloroplatinum complexes of the lead 5-nitro-2-furancarbohydrazide **8** selected from high-throughput screening. Detailed kinetics revealed that the isolated fragments, 5-nitro-2-furancarbohydrazide and cisplatin itself, bind with micromolar affinities at two different subsites of the human enzyme. By tethering both fragments four nitrofuran-based *cis*-diamminedichloroplatinum complexes **13a**−**c** and **20** were synthesized and identified as biligand irreversible inhibitors of the human enzyme with nanomolar affinities. Studies with mutant enzymes clearly demonstrate the penultimate selenocysteine residue as the prime target of the synthesized *cis*-diamminedichloroplatinum complexes.

Introduction

A major obstacle in anticancer chemotherapy is the emergence of drug resistance, leading to a reemergence of a tumor which initially responded well to treatment. *Cis*-diamminedichloroplatinum(II), or cisplatin (cisPt), is a commonly used drug in cancer therapy,[1] particularly prone to resistance, as an increase in dosage is only feasible to a limited extend due to severe toxic side effects. Many of these resistance mechanisms are directly or indirectly linked to the cellular redox system protecting the cells by formation of drug conjugates for export, by counteracting apoptotic signals and by other mechanisms.[2]

One of the key players in the cellular redox system is thioredoxin reductase (TrxR, EC 1.8.1.9).[3] TrxR catalyzes the NADPH-dependent reduction of oxidized thioredoxin ($Trx(S)_2$) according to eq 1:

$$NADPH + Trx(S)_2 \rightleftharpoons NADP^+ + Trx(SH)_2 \quad (1)$$

Thioredoxin (Trx) and TrxR form the thioredoxin system, which is involved in a magnitude of cellular functions,[4] including DNA synthesis and cell signaling, rendering it a suitable target for chemotherapeutic agents per se. Several independent knock-out[5,6,7,8,9] or mutant[10] studies indicate the vital function of both proteins from various species. Furthermore, recent reports provide strong evidence for an important role of the human thioredoxin system in cisPt-resistance.[11]

The catalytic mechanism of large TrxRs is similar to that of glutathione reductase (GR) by sharing similar NADPH- and FAD-binding domains, a dimer interface domain, and the thiol−disulfide redox active center Cys-Val-Asn-Val-Gly-Cys located in the FAD domain of the N-terminal part of each subunit (Scheme 1). The flow of electrons during catalysis is from NADPH to FAD to the active center disulfide and then to the C-terminal redox center formed by a cysteine-selenocysteine couple at the other TrxR subunit. A key feature of the proposed catalytic mechanism of large TrxR is the motion of the flexible C-terminal tail that is responsible for the transport of electrons from the buried N-terminal redox center to large substrates as Trx at the surface of the protein (Scheme 1).[12−16] Data from the three-dimensional structure of mammalian TrxR,[17] and from selective cleavage[13] corroborate this mechanistic model. Beyond the reduction of the natural substrate thioredoxin, the Cys497-Sec498 redox pair reacts with a large variety of structurally diverse low M_r substrates.[3]

* Correspondence to: Elisabeth Davioud-Charvet, delegate of Centre National de la Recherche Scientifique, France, in the frame of a French-German cooperation with the University of Heidelberg, Germany. Phone: +49-6221-54-4188; Fax: +49-6221-54-5586; E-mail: elisabeth.davioud@gmx.de.
† UMR 8525 CNRS-Université Lille II-Institut Pasteur de Lille.
# Giessen University.
|| German Cancer Research Centre.
‡ Université Rennes I.
§ Biochemie-Zentrum der Universität Heidelberg.
⊥ Both authors contributed equally to this work.
⊗ Present address: I.C.P.A.L. 3, rue du Pr Laguesse, BP 83, F-59006 Lille, France.

10.1021/jm050256l CCC: $30.25
Published on Web 10/07/2005

Scheme 1. Postulated Catalytic Mechanism of Human TrxR and Other Large TrxRs for Trx Reduction[3,13,53]

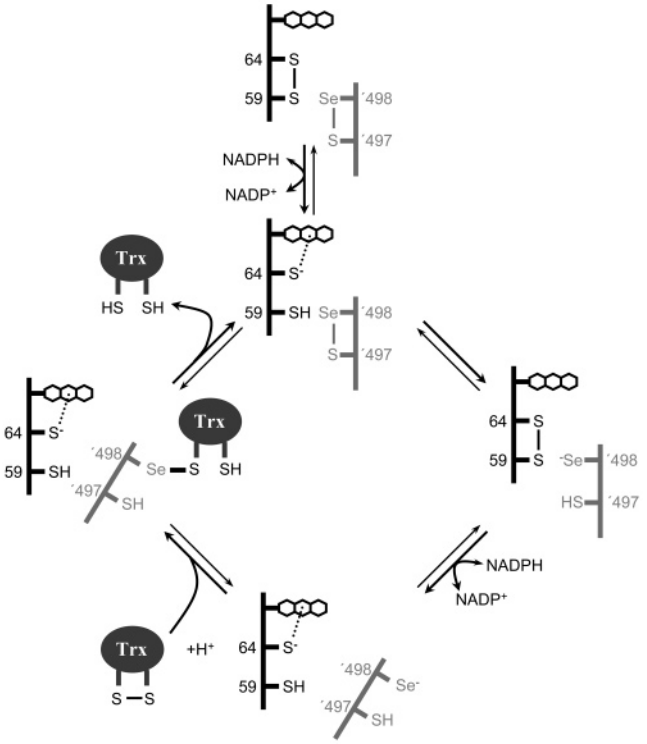

In this sketch, only one reaction center, yet formed by both subunits of the homodimeric mammalian TrxR (indicated by black and gray lines), is shown. The flavin near the N-terminal redox active site (Cys59 and Cys64) is provided by one subunit, and the C-terminal redox active site of the same reaction center by the other subunit (Cys′497 and Sec′498). The oxidized enzyme (E_{ox}) is reduced to an EH_2 species by NADPH.[12] The N-terminal redox active site exchanges the electrons with the C-terminal redox active site of the opposite subunit.[16,31] Additional reducing equivalents provided by NADPH are taken up to yield an EH_4-species.[12] Selective digest experiments suggest that the reduced C-terminal tail now moves to a more solvent exposed position.[13,14] Oxidized thioredoxin reacts with the reduced C-terminal tail's selenolate to yield a mixed selenenyl sulfide, which is cleaved by the adjacent thiol,[31] to yield reduced thioredoxin and the initial TrxR-EH_2 species. Steady-state kinetics demonstrated an overall ping-pong mechanism as indicated by this model.[19] Note *D. melanogaster* TrxR has a disulfide, not a selenenyl sulfide as in mammalian TrxR.

Selenols have a much higher reactivity to bind heavy metal ions than thiols.[18] Therefore, as previously hypothesized, the easily accessible C-terminally located selenocysteine of hTrxR is most likely to be the major target of a variety of more or less effective metal-containing inhibitors.[19,20,21] One of those inhibitors, although rather weak, is cisPt.[11]

As the cellular mode of cisPt action is primarily the formation of covalent adducts with DNA, it may contribute to its effectiveness and to reduction of resistance formation if its specificity toward hTrxR is increased. The optimization of cisPt as hTrxR inhibitor could be reached by following the biligand approach, i.e., linking the cisPt-structure to another moiety that interacts with the N-terminal redox-active site of the enzyme. During catalysis this region can be assumed to be exposed as the reduced C-terminal tail moves toward a more solvent exposed position. The N-terminal interaction might temporarily block the enzyme and should furthermore trap the cisPt-moiety in close proximity to the

Chart 1. Structures of the 5-Nitro-2-furancarbohydrazides **8**, **14b** and Related Derivatives **12a**−**c**, **19** and Their *cis*-Diamminedichloroplatinum Complexes **13a**−**c** and **20** as Inhibitors of Human Thioredoxin Reductase

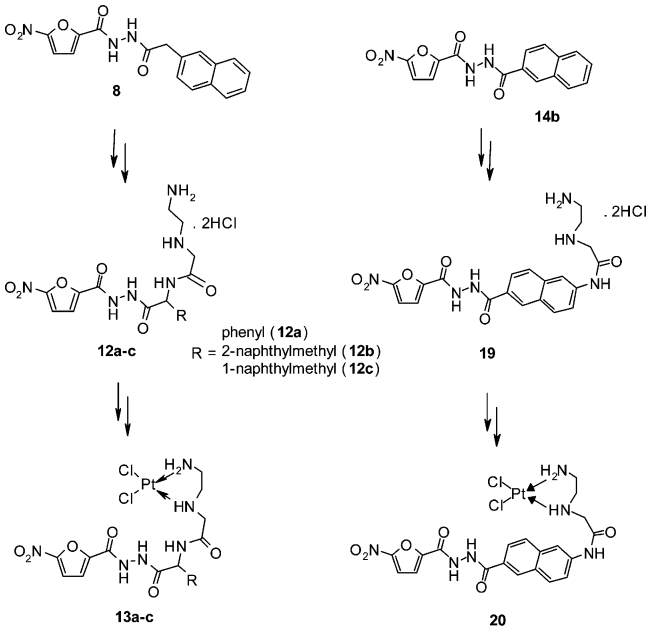

TrxR's unique C-terminal redox center allowing irreversible inhibition. In theory, the advantage of such a bitopic ligand is a more efficient TrxR inhibition than either of the parent compounds alone. The binding affinity of a linked compound is, in principle, the product of the binding constants of the individual fragments plus a term that accounts for the changes in binding affinity that are due to the linker.[22] An additional effect of DNA destruction by cisPt is expected since DNA synthesis and repair depend on the formation of desoxyribonucleotides, which itself is dependent on $Trx(SH)_2$. A synergistic effect should result when taking into account that resistance formation is to some degree dependent on Trx and TrxR. It is noteworthy that many cisPt analogues linked to various DNA ligands to improve DNA-targeting ability, have been described and evaluated,[23−27] although the rationales have been different from the approach proposed here.

In the present paper, the starting lead inhibitor was selected from the primary high-throughput screening of a general library of compounds (unpublished data) in the hTrxR assay using an artificial disulfide substrate, 5,5′-dithiobis(2-nitrobenzamide) (DTNBA).[28] The most active compound was identified to be a 5-nitro-2-furancarbohydrazide derivative **8** with a naphthalene moiety (Chart 1). Various nitroaromatic compounds, including nitrofuran derivatives, are known to bind to several disulfide reductases by acting both as inhibitors and as substrates.[29,30] Starting from the lead structure we report on the synthesis of four platinum-chelating ethanediamine ligands **12a**−**c** and **19** linked to the lead 5-nitro-2-furancarbohydrazide derivative **8** and analogues, and on the inhibitory potency of their corresponding *cis*-diamminedichloroplatinum(II) complexes **13a**−**c** and **20** (Chart 1). The four complexes were synthesized by tethering the nitrofuran moiety to the cisPt moiety with linkers at different positions to the naphthalene group. The binding affinities of these four

complexes for TrxRs were measured in Trx and DTNB disulfide reduction assays and were found to be effective in nanomolar concentrations for irreversible binding to TrxRs. To verify our proposed inhibitory mechanism of the four *cis*-diamminedichloroplatinum(II) complexes **13a**−**c** and **20**, detailed kinetic studies were performed. Apart from the authentic human TrxR, we also included a C-terminally truncated enzyme, a mutant lacking the final 16 amino acids (hTrxRΔ-16) and a Sec→Cys mutant form of hTrxR (Sec498Cys).

As it has previously been shown that the microenvironment of the C-terminal redox center is of importance as well, we included C-terminal mutants of *Drosophila melanogaster* thioredoxin reductase (DmTrxR),[31] a cysteine homologue of the human enzyme, to analyze this aspect with respect to the alkylating properties of the most potent compound **20**.

Results

Inhibitor Screening on hTrxR. In a high-throughput screening 12 000 compounds were analyzed in microtiter plates as potential hTrxR inhibitors at a concentration of 25 μM in the presence of 500 μM NADPH and 200 μM of the artificial disulfide substrate DTNBA.[28] Three known TrxR inhibitors, dichloroindophenol,[32] naphthazarin,[21] and cisPt,[11,33] were selected as references. As judged from the IC_{50} values, only one compound, *N*′-(2-naphthylmethyl)-5-nitro-2-furancarbohydrazide **8** (IC_{50} value =16 μM), was found to be more potent than the three reference inhibitors, dichloroindophenol (IC_{50} = 25 μM), naphthazarin (IC_{50} = 20 μM), and especially cisPt (no inhibition at 25 μM, $IC_{50} \gg 50$ μM) in the TrxR assay using 50 μM DTNBA and 200 μM NADPH. It is noteworthy to mention that any of the intermediates **9a**−**c** to **12a**−**c** and **14a**−**c** to **19**, synthesized after further chemical derivatization of the lead structure **8**, showed IC_{50} values below 40 μM under the same conditions. The most potent TrxR inhibitors, the lead inhibitor **8**, and the four related cisPt analogues **13a**−**c** and **20** were investigated in inhibition studies.

Nitrofuran Reductase Activity of Thioredoxin Reductase. The ability of TrxR to reduce the nitrofuran derivative was studied by following the oxidation of NADPH in the presence of the lead inhibitor **8**. The nitrofuran reductase activity of TrxR was compared with the low intrinsic NADPH oxidase activity of the enzyme in the absence of nitrofuran (NF) (eq 2). TrxR displayed a 21-fold higher NADPH oxidase activity in the presence of 300 μM **8** (eq 3) (0.043 U mg^{-1} protein in the absence versus 0.908 U mg^{-1} protein in the presence of 300 μM nitrofuran **8**).

$$2\ O_2 + NADPH + H^+ \rightarrow 2\ O_2^{-\bullet} + NADP^+ + 2H^+ \quad \text{(enzymatic)} \quad (2)$$

$$2\ NF + NADPH + H^+ \rightarrow 2\ NF^{-\bullet} + NADP^+ + 2H^+ \quad \text{(enzymatic)} \quad (3)$$

The K_m (529 ± 80 μM) and k_{cat} (2.5 ± 0.3 s^{-1} per catalytic subunit) values were derived from measurements at seven different substrate concentrations. Following NADPH consumption, **8** was reduced by TrxR with a catalytic efficiency k_{cat}/K_m of 4.7 × 10^3 M^{-1} s^{-1}. The data are in good agreement with previous observations made with nitrofuran and nitrophenyl derivatives,[30,34] which possess single-electron reduction potentials between −255 and −287 mV.

Characterization of Inhibition by Lead Compound 8 in the Steady-State. To compare the binding of the inhibitor to the N- and/or the C-terminal parts of TrxR, these studies were done using the wild-type enzyme (wt-hTrxR) and the truncated enzyme (hTrxRΔ-16) lacking the second redox center (deletion of 16 amino acids). The suitable TrxR assay based on Trx reduction could not be used because Trx is only reduced at the C-terminal redox center of wild-type enzyme. Thus, DTNB was selected as artificial substrate to allow comparison of the inhibition type of the lead compound **8** with wild-type TrxR and truncated enzyme. DTNB is known to be reduced at both active sites of wild-type enzymes, e.g. of *Plasmodium falciparum* TrxR, but with 14-fold reduced catalytic efficiency k_{cat}/K_m at the N-terminal part.[35] This mainly resulted from higher K_m value for DTNB and reduced k_{cat}, as suggested from the determined K_m and k_{cat} values for DTNB reduction at the N-terminal binding site of the human truncated TrxR. Using eight different substrate concentrations (11−435 μM) in the absence of inhibitor, DTNB is reduced by hTrxRΔ-16 with K_m and k_{cat} values of 5305.9 ± 67.5 μM and 0.79 s^{-1}, versus values of 50.5 ± 1.6 μM and 20.79 s^{-1}, when reduced by wt-hTrxR. This accounts for a 2825-fold reduced catalytic efficiency k_{cat}/K_m at the N-terminal part of the human enzyme.

Lead Compound 8 Follows Uncompetitive Kinetics in Inhibition of Wild-Type Human TrxR. To investigate the outcome of wt-hTrxR inhibition at varying DTNB concentrations (11−435 μM), kinetics were first performed using saturating NADPH concentration (200 μM) in the presence of inhibitor **8** (0−40 μM). The experimental data for wild-type enzyme were analyzed using eq 4 for uncompetitive inhibition (Figure 1A), where [S] is the concentration of varied substrate, [I] is the inhibitor concentration, V_{max} is the maximal velocity, K_m is the Michaelis−Menten constant, and K_i is the inhibition constant for I binding to the ES complex.

$$v = \frac{V_{max}[S]}{K_m + [S]\left(1 + \frac{[I]}{K_i}\right)} \quad (4)$$

The K_i value of 16.0 ± 0.8 μM for compound **8** was determined as shown in Figure 1 (see inset in Figure 1A). The Cornish−Bowden plot (Figure 1B) as well as the Dixon (Figure 1C) and Lineweaver−Burk (Figure 1D) plots for compound **8** was consistent with uncompetitive inhibition type, whereas expressions for competitive and noncompetitive inhibition could not accurately describe the observed relationship between K_i and DTNB concentration. Under steady-state conditions, it clearly appeared from the Cornish−Bowden plot (Figure 1B) that binding of the inhibitor was facilitated by DTNB binding, revealing an induced cooperative effect. A detailed analysis of this plot showed that, as DTNB concentration increases, the constant K_i for the dissociation of I appeared by itself in a slope and reached a maximum, approximately 12 μM, when [DTNB] is in the K_m range (see inset in Figure 1A).

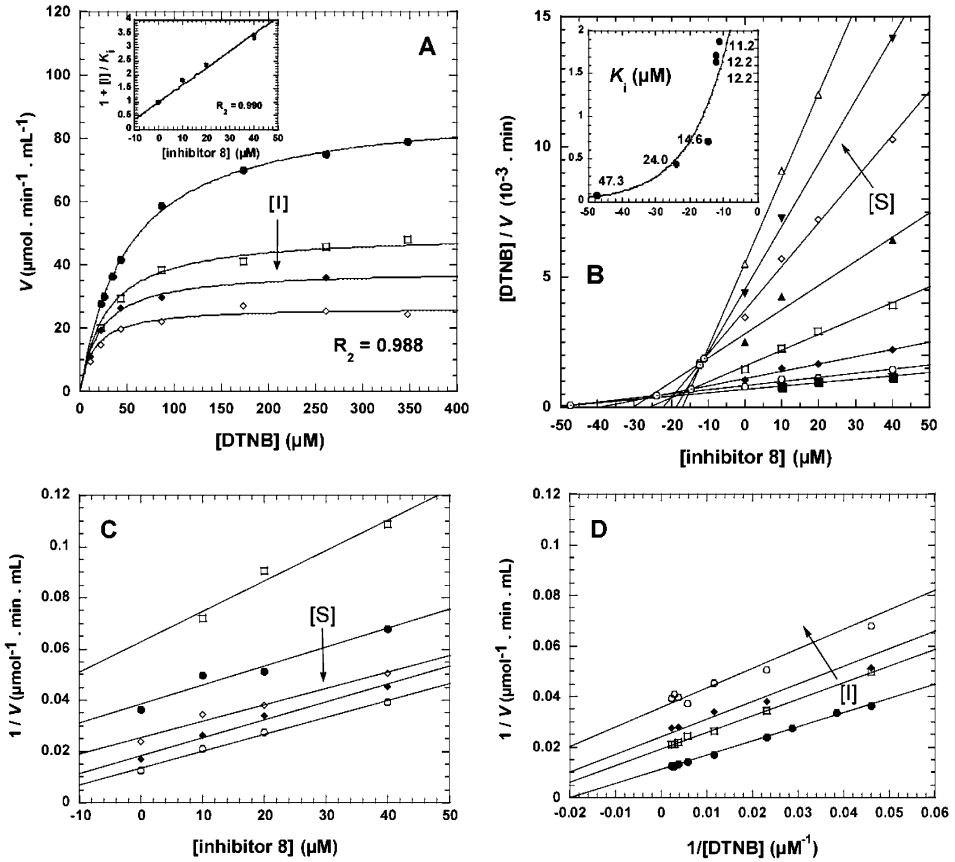

Figure 1. Characterization of the inhibition type of wild-type human placenta thioredoxin reductase by lead nitrofuran compound **8** in the steady-state. Inhibition of wild-type human placenta thioredoxin reductase by the lead derivative **8** in DTNB reduction assay was characterized (Panel A), and the K_i value was determined (inset). Uncompetitive type of inhibition was confirmed by Cornish−Bowden, Dixon, and Lineweaver−Burk plots (Panels B, C, D). DTNB concentrations were 10.9, 21.7, 43.4, 86.9, 173.8, 260.9, 347.6, and 434.5 μM. Inhibitor concentrations used were 0, 10, 20, and 40 μM.

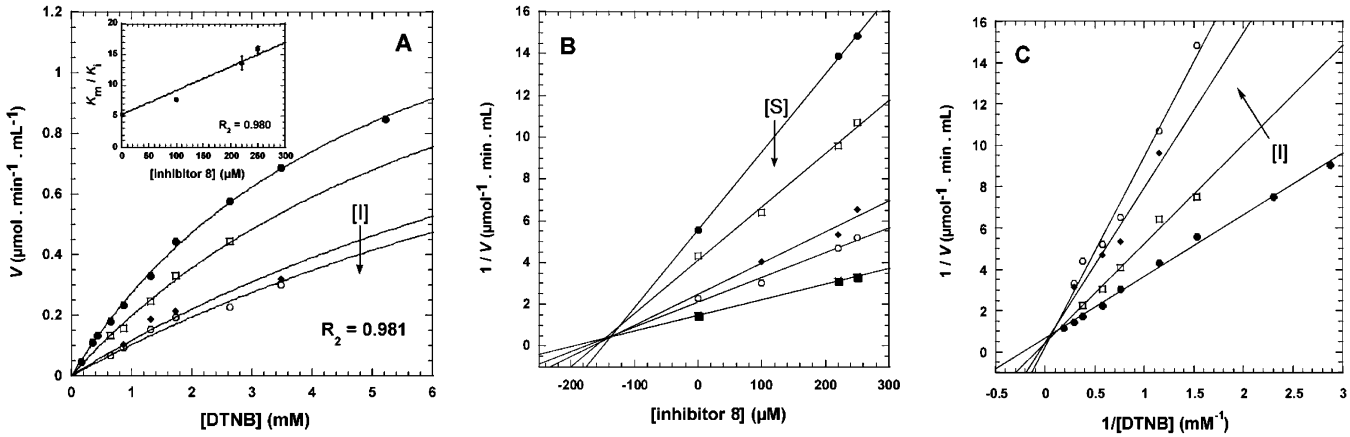

Figure 2. Characterization of the inhibition type of truncated human placenta thioredoxin reductase by lead nitrofuran compound **8** in the steady-state. Inhibition of truncated human placenta thioredoxin reductase by the lead derivative **8** in the DTNB reduction assay was characterized (Panel A), and the K_i value was determined (inset) by fitting the experimental data to the Michaelis−Menten equation. Competitive type of inhibition was confirmed by Dixon and Lineweaver−Burk plots (Panels B and C). DTNB concentrations were 0.17, 0.35, 0.43, 0.65, 0.87, 1.32, 1.74, 2.63, 3.48, and 5.21 mM. Inhibitor concentrations used were 0, 100, 220, and 250 μM.

Lead Compound 8 Follows Competitive Kinetics in Inhibition of Truncated Human TrxR. Due to the much higher $K_{m\ DTNB}$ value for the truncated enzyme hTrxRΔ-16, it was possible to study the inhibition of hTrxRΔ-16 by varying the DTNB concentration at higher concentration level (0.6−6.0 mM). Kinetics were performed using saturating NADPH concentration (200 μM) in the absence or in the presence of inhibitor **8** (0−250 μM). Assuming simple competitive inhibition, the data were fitted to eq 5 (Figure 2A):

$$v = \frac{V_{max}[S]}{K_m\left(1 + \frac{[I]}{K_i}\right) + [S]} \quad (5)$$

The K_i value for **8** was determined as 136.5 ± 9.9 μM with respect to DTNB (see inset in Figure 2A). The

Chart 2. Structures of the Four Amino Acids: Phenylglycine (**21**), 2-Naphthylalanine (**22**), 1-Naphthylalanine (**23**), 6-Amino-2-naphthoic Acid (**24**)

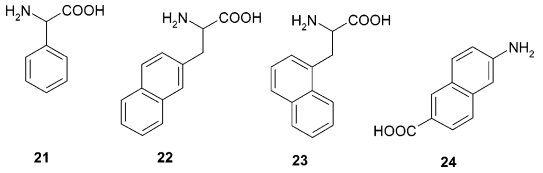

21 22 23 24

competitive type of inhibition of hTrxRΔ-16 by **8** was derived from Dixon (Figure 2B) and Lineweaver−Burk (Figure 2C) plots. At this stage, it was already obvious that the kinetics were more complex (weakly sigmoidal at low inhibitor concentration as DTNB concentration increased) and a better curve fit was realized by using the equation for inhibition of multisite-enzymes (data not shown). The plot K_m/K_i versus [I] could indeed be interpreted using an exponential equation. This observation was further confirmed with complex **20** in the following kinetics where marked sigmoidal curves were obtained and could be fully analyzed.

Chemistry. From the selected lead structure **8**, the *N*′-(2-naphthylmethyl)-5-nitro-2-furancarbohydrazide, two series of analogues **9a**−**c** and **14a**−**c**, as well as the related ethanediamine ligands **12a**−**c** and **19**, and their corresponding *cis*-diamminedichloroplatinum(II) complexes **13a**−**c** and **20** (Chart 1) were synthesized. The design of the four cisPt complexes was oriented as followed. Assuming that the C-terminal part of TrxR moves to the external surface of the protein in the course of the catalytic cycle, a rational approach is to design a bitopic and irreversible TrxR inhibitor that would (i) be recognized by the enzyme in a first sub-site, (ii) anchored by multiattachment in a second subsite revealed after motion of the C-terminal part, and (iii) react with the exposed selenocysteine. For this purpose, a coordinating arm linking the 5-nitro-2-furancarbohydrazide moiety to the cisPt unit is required. The selected suitable arm consists of a spacer that ends by a chelating ethylenediamine function. The linkage of the arm to the 5-nitro-2-furancarbohydrazide was built as followed. The methylene bridge of the 2-naphthylmethyl substituent in the lead structure **8** was selected to anchor the suitable arm. To give more flexibility to the spacer the homo analogue was built by starting from the racemic amino acid 2-naphthylalanine **22** (Chart 2) instead of a 2-naphthylglycine. The regioisomer 1-naphthylalanine **23** was also selected as starting material to vary the flexibility of the spacer. Then the phenylglycine **21** was selected in order to evaluate the essential requirement of the naphthyl moiety for optimal binding to the target. Finally, the 6-amino-2-naphthoic acid **24** allowed the building of a more flexible and "linear" spacer between the 5-nitro-2-furancarbohydrazide unit and the chelating ethylenediamine function.

Our starting hTrxR inhibitor compound **8** was obtained according to standard procedures for peptide synthesis in solution (Scheme 2). Briefly, 5-nitro-2-furoic acid was reacted with *tert*-butyl carbazate using PyBOP as coupling agent. The Boc group was removed by methanolic HCl solution resulting in 5-nitro-2-furancarbohydrazide hydrochloride **7**, which was coupled with 2-naphthyl acetic acid to yield diacylhydrazine **8**.

To obtain the platinum complexes **13a**−**c** and **20**, we first prepared the protected N^{α}-(ω-aminoethyl)amino acid **5** as a building block. The synthesis of the polyamino acid side chain is outlined in Scheme 3 and is based on previously published protocols with slight modifications.[36] We used the benzyl (*N*-benzyl or benzyl ester) and the *N*-*tert*-butoxycarbonyl moieties as protecting groups. The first step was carried out to selectively protect the ethylenediamine. Double acylation was avoided by using a large excess of the nucleophilic amine and purification yielded the monoprotected *N*-Boc ethylenediamine **1** with 65% yield. The resulting amine **2** was used in a reductive amination reaction with benzaldehyde and sodium borohydride. This temporary protection of amine **2** by the *N*-benzyl protecting group allowed in the next step the monosubstitution of amine **3** by 2-benzyl bromoacetate, hence preventing polyalkylation of amine **2**. Catalytic hydrolysis using ammonium formate and Pd (10% on charcoal) was applied to remove the *N*-benzyl and the Z-protected ester. Zwitterion **4** was finally protected by an *N*-*tert*-butoxycarbonyl moiety and compound **5** which contains two equal *N*-protected groups was used directly as a building unit for the design of the platinum complexes.

Different Pt chelating ligands were investigated, assuming that the locus where the linker chain is attached can position the platinum atom in quite different ways with respect to the potential nucleophilic attack from the selenocysteine during the enzyme catalytic cycle. To attach the platinum-chelating ethanediamine linker at different *loci* of the 5-nitro-2-furancarbohydrazide core, we selected four differently substituted (three naphthyl- and one phenyl-) amino acids **21**−**24** (Chart 2) to design the four Pt-ligands **12a**−**c** and **19**, and their corresponding *cis*-diamminedichloroplatinum(II) complexes **13a**−**c** and **20**. The phenylamino acid **21** was chosen to evaluate the importance of the naphthalene moiety for hTrxR recognition.

The 5-nitro-2-furancarbohydrazides **9a**−**c** were prepared by coupling the three racemic *N*-Boc amino acids using the standard PyBOP methodology (Scheme 2). After deprotection of the Boc group, the amines **10a**−**c** were next coupled with the polyamino acid **5** to yield **11a**−**c**. Their Boc groups were removed by methanolic HCl solution, and the platinum complexes **13a**−**c** were obtained by titrating the racemic polyamine hydrochloride **12a**−**c** in the presence of equimolar amounts of K_2PtCl_4 in DMF/H_2O (1:3). Using this aqueous DMF solution significantly increased the efficiency of the platination reaction compared to the commonly used aqueous methanol mixture. The last two steps of the platinum synthesis were monitored by analytical HPLC. For the synthesis of the cisPt complex **20** (Scheme 4), the aromatic amine **17** was first prepared by coupling the 5-nitro-2-furancarbohydrazide **7** and the *N*-Boc-naphthoic acid **15** in the presence of PyBOP. PyBOP was also used as coupling agent for the synthesis of **14a**−**c**, the three analogues of **8**. The deprotection of the Boc group in **16** was carried out by using TFA in CH_2Cl_2 and the coupling reaction of **17** with the *N*-protected ethanediamine linker **5** was achieved in DMF in the presence of PyBROP to produce **18**. The last two reactions to produce **20** were performed in a way similar to that used for **13a**−**c**. The conditions of complexation

Scheme 2. Synthesis of 5-Nitro-2-furancarbohydrazide Derivatives[a]

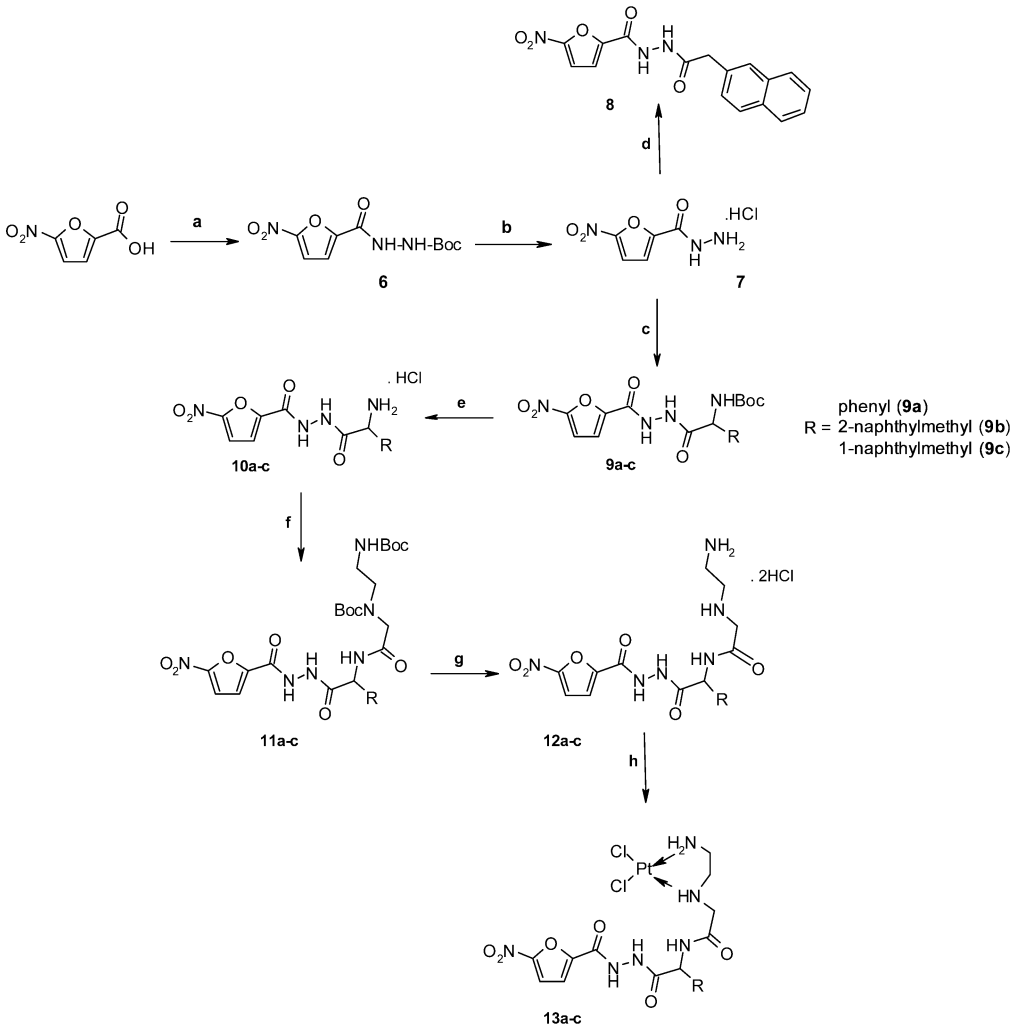

[a] Reagents and conditions: (a) PyBOP, DIEA, *tert*-butyl carbazate, CH_2Cl_2, rt, 16 h; (b) MeOH, HCl, rt, 16 h; (c) PyBOP, DIEA, CH_2Cl_2, *N*-Boc-amino acid, rt, 16 h; (d) PyBOP, DIEA, CH_2Cl_2, 2-naphthylacetic acid, rt, 16 h; (e) MeOH, HCl, rt, 16 h; (f) PyBOP, DIEA, CH_2Cl_2, compound **5**, rt, 24 h; (g) MeOH, HCl, rt, 16 h; (h) K_2PtCl_4, DMF/H_2O 1:3, rt, 10 days.

Scheme 3. Synthesis of Polyaminocarboxylic Acid **5**[a]

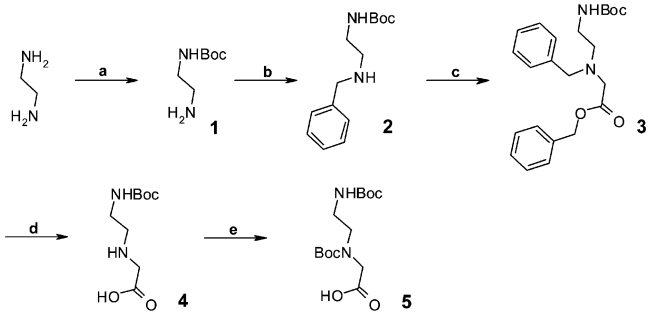

[a] Reagents and conditions: (a) $(Boc)_2O$, CH_2Cl_2, 0 °C, 3 h and room temperature, 16 h; (b) (1) PhCHO, NEt_3, MeOH, molecular sieves 3 Å, rt, 0 °C, 4 h, (2) $NaBH_4$, MeOH, rt, 16 h; (c) 2-benzyl bromoacetate, DIEA, DMF, 0 °C, 1 h; (d) ammonium formate, Pd/C, MeOH, reflux, 16 h; (e) $(Boc)_2O$, NaOH, dioxane/H_2O 4:1, rt, 16 h.

by K_2PtCl_4 were slightly modified by performing the titration of diamine **19** at 60 °C to accelerate the reaction. Once prepared, the cisPt complexes appeared insoluble in water and MeOH, but dissolved rapidly in DMF and DMSO. DMF was used as solvent for the NMR and enzymic studies, as well as in all enzymatic and biological studies, because, as previously reported, the high reactivity of DMSO toward platinum complexes is responsible for slow chloro-ligand−DMSO exchange.[27]

From the proton NMR spectra, the signal corresponding to the amine group of ethylenediamine appeared strongly deshielded in the complexes (δ between 3.00 and 3.46 ppm for NH and δ between 2.50 and 3.40 ppm for NH_2). After complexation by K_2PtCl_4, we also observed 50:50 diastereoisomeric mixtures, due to the racemic parent polyamine and to δ and λ enantiomers of the 1,2-diaminoethane ring, that can adopt an envelope conformation, for the three Pt complexes **13a**−**c**, both from HPLC chromatograms and NMR spectra. By contrast, the case did not apply for the Pt complex **20** starting from the nonracemic diamine **19**. The ^{195}Pt NMR spectra were obtained for the four complexes and showed ^{195}Pt resonances at δ values of ca. −2346 ppm (from $PtCl_6^{2-}$). These values are in the same range as those exhibited by previously reported ethylediamine-linked Pt complexes in accordance with the mode of coordination of the platinum.[24,25] The geometry of complexes is also supported by FTIR spectroscopy. The IR spectral data showed bands for **13a**−**c** at 477 and for **20** at 474.4 cm^{-1} assigned to ν(Pt−N). The stoichiometry of platinum in the complexes **13a**−**c** and **20** was measured by high resolution inductively coupled plasma-

Scheme 4. Synthesis of 5-Nitro-2-furancarbohydrazide Derivatives **14a**−**c**, **16**−**20**[a]

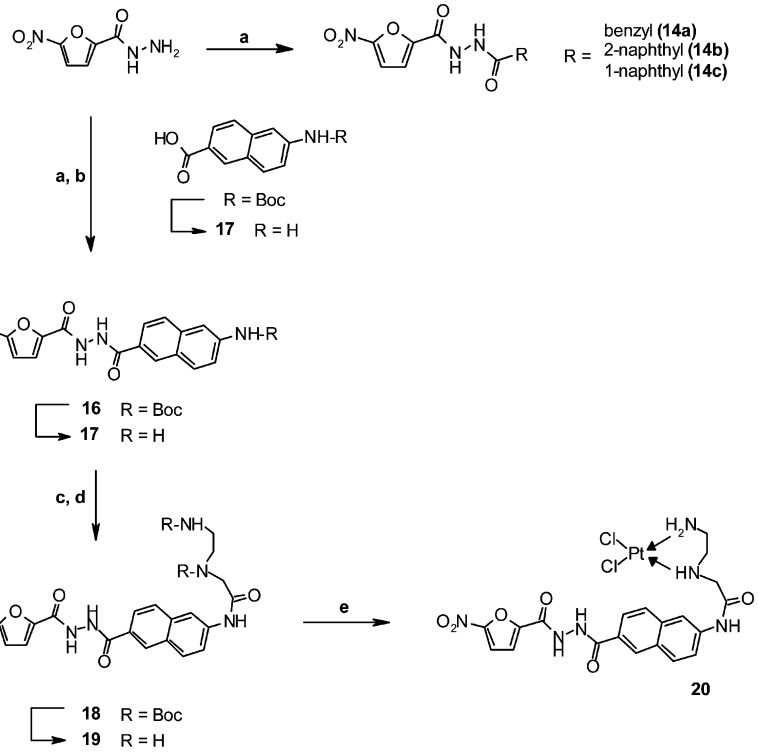

[a] Reagents and conditions: (a) appropriate acid, PyBOP, DIEA, CH_2Cl_2, rt, 16 h; (b) CH_2Cl_2, TFA, rt, 16 h; (c) PyBROP, Compound **5**, DIEA, DMF, rt, 16 h; (d) MeOH, HCl, rt, 72 h; (e) K_2PtCl_4, DMF/H_2O 1:3, 60 °C, 7 days.

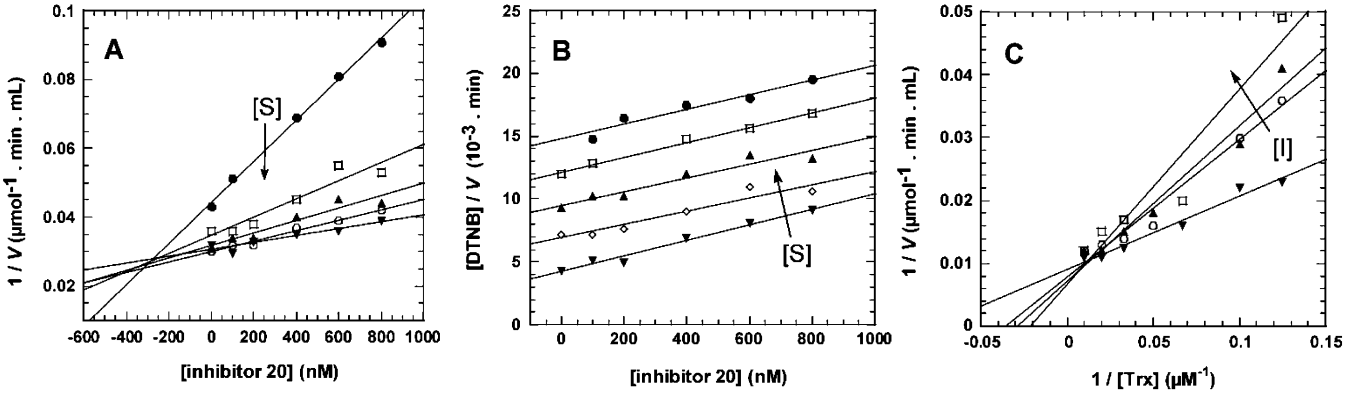

Figure 3. Characterization of the inhibition of wild-type human placenta thioredoxin reductase by CisPt Complex **20** in the steady-state. Inhibition of wild-type human placenta thioredoxin reductase by CisPt Complex **20** was characterized in the DTNB reduction assay (Panels A and B) and the Trx reduction assay (Panel C). Competitive type of inhibition of wt-hTrxR in DTNB reduction assay was evidenced from Dixon and Cornish−Bowden plots (Panels A and B). DTNB concentrations were 100, 200, 300, 400 and 500 μM. Inhibitor concentrations used were 0, 100, 200, 400, 600 and 800 nM. Panel A. The intersection point of all lines in the upper left quadrant from Dixon plot, as typical for competitive inhibition, indicates a K_i value of 275 nM by extrapolation to the abscissa. Panel B. The reversible competitive component of inhibition becomes evident by parallel linear regression curves from the Cornish−Bowden plot. Panel C. The type of inhibition of wt-hTrxR by inhibitor **20** measured in Trx assay is complex, as suggested from the Lineweaver−Burk plot showing the intersection point of the lines in the upper right quadrant (upper to lower lines are for 500, 250, 125, 20 nM inhibitor **20**). Trx concentrations were 8.0, 10.0, 14.9, 20.0, 30.3, 50.0, and 100.0 μM.

mass spectrometry (ICP-MS).[37] Four samples corresponding to Pt-complexes **13a**−**c** and **20** were prepared at fixed concentration and analyzed. Platinum concentration was determined by ICP-MS for **13a**−**c** and **20** solutions and was confirmed by comparison with calibrated platinum reference solutions.

Steady-State Kinetic Analysis of the Complexes. The reversible inhibitory properties of the compounds were analyzed in direct assays under steady-state conditions, using either thioredoxin or the alternative disulfide DTNB as substrate. All assays were started by the addition of NADPH in order to minimize effects caused by prereduction of the enzyme. The amount of enzyme was kept low in order to render the nitrofuran reduction negligible. As indicated by Dixon ($1/v$ versus [I], Figure 3A) and Cornish−Bowden ([S]/v versus [I], Figure 3B) plots, all compounds exhibited competitive type inhibition with respect to DTNB reduction. The respective K_i values for competitive inhibition were derived from the plots and calculated using eq 5.

The K_i values were 110 nM for compound **13a**, 84 nM for **13b**, 120 nM for **13c**, and 275 nM for compound **20**.

Table 1. Time-Dependent Inhibition of Wild Type hTrxR and hTrxR Sec498Cys Mutant by *cis*-Diamminedichloroplatinum Complexes **13a**−**c** and **20** (IC_{50} values)[a]

IC_{50} (μM)	**8**	**13a**	**13b**	**13c**	**20**
wt-hTrxR Trx assay	nd	0.16	0.14	0.21	0.12
wt-hTrxR DTNB assay	18	0.10	0.03	0.08	0.11
Sec498Cys Trx assay	nd	~250[b]	24.0	21.0	38.0
Sec498Cys DTNB assay	nd	265	230	235	130
hTrxRΔ−16 DTNB assay	215	520	195	170	145
hGR	4.1	2.6	0.95	1.0	1.0

[a] DTNB assay: 5 nM wild-type hTrxR and 100 nM mutant hTrxR, respectively, were preincubated for 10 min at 25 °C in phosphate buffer in the presence of 200 μM NADPH with or without inhibitor; the reaction was started by adding 3 mM DTNB. Trx assay: 30 nM wild-type hTrxR and 1.3 μM mutant hTrxR, respectively, were preincubated for 10 min at 25 °C in assay buffer in the presence of 100 μM NADPH with or without inhibitor; the reaction was started by adding 20 μM hTrxC72S. DMF was used in the control assays. All values are mean values of at least three independent determinations which differed by less than 15%. [b] Compound **13a** showed a strong absorbance at 340 nm which limited exact IC_{50} determination.

These values revealed that the 2-naphthylmethyl unit was the optimal substituent recognized by hTrxR in agreement with the substitution pattern of the lead structure **8**. The results obtained with thioredoxin as substrate were more complex (Figure 3C). Dixon, Cornish−Bowden, and Lineweaver−Burk curves of inhibited wild-type and mutant (Sec498Cys) hTrxR showed an intersection point in the upper right quadrant**,** but a clear classification of inhibition type was not possible.

In the presence of compound **13c** and in the absence of any disulfide substrate, the Sec498Cys hTrxR mutant showed a strong NADPH oxidation reaction (20 mU/mg), but not in the control assay with DMF instead of inhibitor, which is most likely due to an induced oxidase activity of the alkylated enzyme. This effect had been previously observed with 1-chloro-2,4-dinitrobenzene-alkylated human thioredoxin reductase.[38]

Relative IC_{50} Values from Time-Dependent Inactivation. A general feature of disulfide reductases is their particular susceptibility toward many nucleophilic compounds in the NADPH-reduced state. This holds true for TrxR. Less than 10% inhibition was observed when the wild-type enzyme was preincubated with the compounds in the absence of NADPH. For comparable results we incubated the enzyme for 10 min with NADPH and inhibitor and started the assay by adding the respective disulfide substrate. Apart from wt-hTrxR we also analyzed the hTrxR mutant (Sec498Cys) and the truncated hTrxRΔ-16 enzyme to verify the preferential effects on selenocysteine at the C-terminal redox center. Inhibition of the closely related enzyme human glutathione reductase (hGR, EC 1.8.1.7.) was also determined to analyze enzyme specificity toward inhibitors. The IC_{50} values for the four compounds **13a**, **13b**, **13c**, and **20** were calculated from dose−response curves and are summarized in Table 1. The IC_{50} values of the lead 5-nitro-2-furancarbohydrazide derivative **8** were added for comparison. Under the same conditions, no time-dependent inhibition of the enzyme was observed in the presence of the reversible hTrxR inhibitor **8**. Wild-type hTrxR was inhibited by all four complexes in the nanomolar range (IC_{50} values from 30 nM to 110 nM in DTNB reduction assay; 120 nM to 210 nM in Trx reduction assay). These IC_{50} values found in the submicromolar range in wt-hTrxR assays revealed complex **20** as the most effective for inactivation. The flexibility of the spacer introduced in complex **20** seems to play an important role in the rate of the reaction between the cisPt unit and the selenocysteine of this enzyme. The inhibition of the mutant (Sec498Cys) hTrxR was by at least 2 orders of magnitude less effective. This result strongly supports the hypothesis that platinum complexes interact specifically with the selenocysteine at the C-terminal Cys-Sec redox pair. Interestingly, the inhibition of the mutant was more effective in the presence of its natural substrate Trx than in the presence of DTNB, an observation that will be discussed below. The IC_{50} values of the four investigated compounds were found to be 5 to 16-fold higher in the hGR than in the hTrxR assays, indicating a relative TrxR specificity for our compounds.

Reversibility studies of the inhibited hTrxR were tested for all four compounds. After a 10 min-incubation period of hTrxR with 2 μM inhibitor in the presence of 100−200 μM NADPH more than 90% of all enzyme molecules were inhibited. Addition of 10 mM dithiothreitol (DTT) for 2 h and exhaustive dialysis did not restore TrxR activity (less than 5%). This suggests that the inhibition is irreversible and that the formation of a stable covalent bond between the enzyme and the inhibitor is involved in the inactivation process.

Time-Dependency and Irreversibility of Inhibition of hTrxR. As shown above, it was confirmed that NADPH-reduction is a prerequisite for irreversible TrxR inhibition by cisplatinum complexes. On incubation with the complexes, human TrxR is inhibited in a time-dependent manner and the inhibition follows pseudo-first-order kinetics. The process for enzyme inactivation may be represented by the following eq 6:

$$S_N\text{-}\mathbf{E}\text{-}S_C + I \rightleftharpoons [S_N\text{-}\mathbf{E}\text{-}S_C\bullet I] \overset{K_{I,S_C}}{\rightleftharpoons} [S_N\text{-}\mathbf{E}^*\text{-}S_C\bullet I] \overset{K_{I,S_N}}{\rightleftharpoons} [{}^*\mathbf{E}\begin{matrix}S_C\\ S_N\end{matrix}\bullet I] \xrightarrow{k_i} [S_N\text{-}\mathbf{E}^*\text{-}S_C\text{–}I] \quad (6)$$

$K_{I,SN}$ represents the dissociation constant of the inhibitor at the N-terminal redox active site, and $K_{I,SC}$ the corresponding constant at the C-terminal redox active site, respectively. k_i is the first-order rate constant for irreversible inactivation. It is however unlikely that both parts of the inhibitor are firmly bound to the enzyme simultaneously. The main function of the nitrofuran moiety is to guide the cisPt-ligand to its site of action and to trap it there until the reaction with the selenolate has taken place. In good accordance with the experimental data, this setting allows to apply the derivation by Kitz and Wilson,[39] for irreversible inactivation. Under the assumption that the concentration of inhibitor (I) is much higher than the stoichiometric amount of enzyme (E_0), it is possible to calculate the remaining amount of active enzyme (E) at time t via eq 7, according to the derivation by Kuo and Jordan:[40]

$$\frac{\ln\left(\frac{E}{E_0}\right)}{t} = -k_{obs}(t) = \frac{k_i}{1 + K_{I,SN}[I]^{-1} + K_{I,SN}K_{I,SC}[I]^{-2}} \quad (7)$$

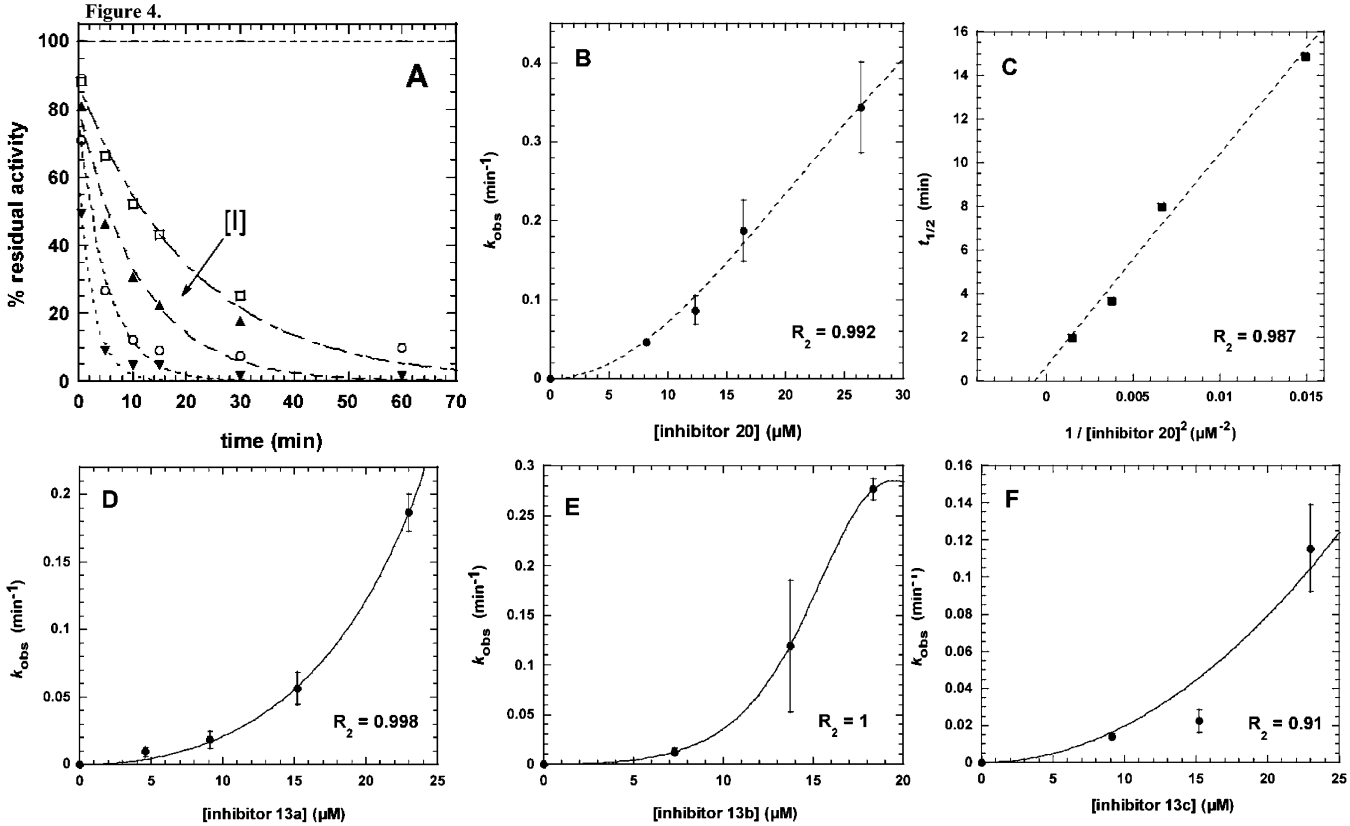

Figure 4. Time-dependent inactivation of wild-type human thioredoxin reductase by CisPt Complexes **20** and **13a**−**c**. The time-dependency of inactivation of wild-type hTrxR is shown in Panels A−C for CisPt complex **20**, in Panel D for CisPt complexes **13a**, in Panel E for **13b**, and in Panel 4F for **13c**. Panels A−C: Different aliquots of pretreated wt-hTrxR enzyme were tested for residual activity at different time periods: 0.5, 5, 10, 15, 30, and 60 min. Data for inhibitor **20** are presented in the primary plot from Panel A. The dissociation constants for inhibitor **20** from the N-terminal redox active site and from the C-terminal redox active site ($K_{I,SN}$, $K_{I,SC}$), respectively, and the first-order rate constants for irreversible inactivation k_i were determined. The k_{obs} data versus [I] were fitted to the eq 7 in the text, resulting in the plot given in Panel B. The $t_{1/2}$ values versus 1/[inhibitor]$^{-2}$ were fitted to the eq 8 in the text, resulting in the plot given in Panel C. Inhibitor **20** concentrations used were 0, 8.2, 12.3, 16.4, and 24.6 μM. Panels D: Inhibitor **13a** concentrations used were 0, 4.6, 9.1, 15.2, and 23.0 μM. Panels E: Inhibitor **13b** concentrations used were 0, 7.3, 13.7, and 18.3 μM. Panels F: Inhibitor **13c** concentrations used were 0, 9.1, 15.2, and 23.0 μM.

The observed $t_{1/2}$ for each concentration of inhibitor is given by eq 8:

$$t_{1/2} = t^{\infty}_{1/2}(1 + K_{I,SN}\cdot[I]^{-1} + K_{I,SN}K_{I,SC}\cdot[I]^{-2}) \quad (8)$$

where $t^{\infty}_{1/2} = (\ln 2)/k_i$.

The primary plot (% residual activity versus pre-incubation time) defining time-dependent inhibition of wild-type hTrxR is shown in Figure 4A. At early stages, the inactivation occurred by a pseudo-first-order process following eq 7 (Figure 4B). In the later stages, the inactivation kinetics became distinctly sigmoidal (as shown e.g. for inhibitor **13b** in Figure 4E). In accordance with eq 8, a secondary plot of $t_{1/2}$ (obtained from the early stages of inactivation) against [I]$^{-2}$ resulted in a linear relationship at low concentration of inhibitor **20** (Figure 4C). For inhibitor **20**, a first-order rate constant k_i of 0.96 min^{-1} as well as $K_{I,SC}$ and $K_{I,SN}$ dissociation constant values of 30 nM and of 42 mM were determined from plots in Figure 4A,B. The inactivation process of hTrxR by the other cisPt complexes **13a**−**c** obeyed the same eq 7 (Figures 4D−F).

Effects on *Drosophila melanogaster* Thioredoxin Reductase. The results shown above indicate that our cisPt complexes act as active site-directed irreversible inhibitors as expected. From data gathered with the mutant (Sec498Cys) hTrxR, it was assumed that the very reactive C-terminal selenolate of wt-hTrxR attack the platin atom of the *cis*-diamminedichloroplatinum(II) moiety of **13a**−**c** and **20**. In the case of *Drosophila melanogaster* enzyme (DmTrxR) the serine residues flanking the C-terminal Cys residues are responsible for activating the Cys to match the catalytic efficiency of a Sec-Cys pair as found in hTrxR.[31] This is due to the low pK_a values of the selenol in hTrxR[41] and the decreased pK_a of Cys in wild-type DmTrxR. Consequently, a variation in the pK_a value of the cysteines in wild-type and mutant DmTrxRs should influence the concentration of the nucleophilic thiolates and thereby the effectiveness of the inhibitor complexes. To validate this assumption, the reactivity of the most potent inhibitor **20**, with respect to alkylation, was compared in assays with wild-type recombinant *D. melanogaster* enzyme and C-terminal mutants.[31] In these mutants, either the critical Cys was replaced by a Sec (Cys490Sec), or the surrounding serine residues in the wild-type enzyme (SCCS) were replaced by glycines (GCCG), a residue found in the human C-terminal active center (GCUG). As shown previously,[31] the flanking polar serine residues at the C-terminal Cys-Cys-redox active site enhance the cysteine reactivity significantly compared to the nonpolar glycine mutants. The prereduced

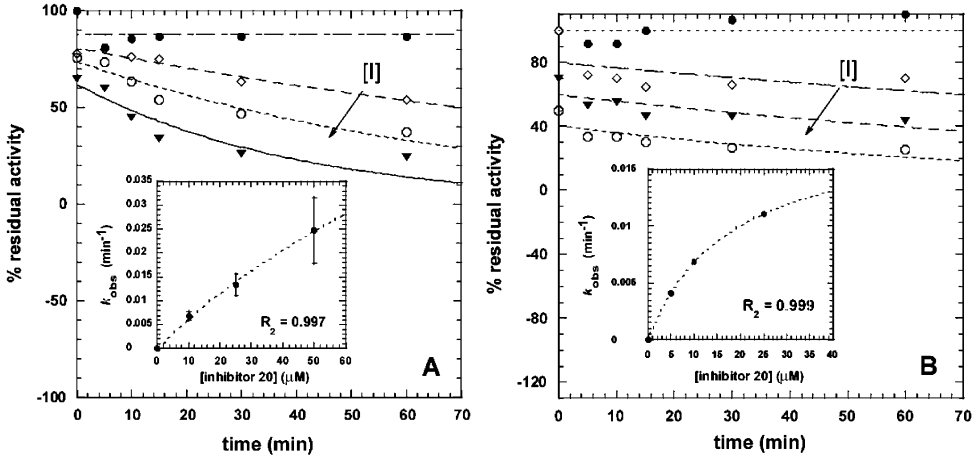

Figure 5. Time-dependent inactivation of wild-type *D. melanogaster* thioredoxin reductase and of SCUS mutant by CisPt complex **20**. The time-dependency of inactivation of wild-type DmTrxR and of SCUS mutant is shown in Panels A and B for CisPt complex **20**, respectively. Different aliquots of pretreated wt-hTrxR enzyme were tested for residual activity at different time periods: 0, 5, 10, 15, 30, and 60 min. Panel A: Inhibitor concentrations used were 0, 10, 25, and 50 μM. Panel B: Inhibitor concentrations used were 0, 5, 10, and 25 μM.

enzymes were inactivated in a time- and concentration-dependent manner. The wild-type (SCCS) enzyme was inactivated the fastest, the GCCG-mutant the slowest, as predicted. Detailed kinetics are given below.

Inhibition by the four complexes **13a**−**c** and **20** followed pseudo-first-order reaction kinetics. A semilogarithmic plot of the fraction of noninhibited enzyme activity $\ln(v_i/v_0)$ versus preincubation time yielded linear curves with increasing slopes, equivalent to the apparent rate constant of irreversible inhibition (k_{obs}). The k_{obs} values for **20** and wild-type enzyme ranged between 6.9×10^{-3} min^{-1} and 24.7×10^{-3} min^{-1} within the log-linear range of the inhibition curve, and a maximal k_i value of 1.7×10^{-3} s^{-1} (Figure 5A). A double reciprocal replot of k_{obs} versus [I] was fitted to the linear relationship (eq 9):

$$k_{obs} = \frac{k_i[I]}{K_I + [I]} \quad (9)$$

The secondary plots expressing k_{obs} as a function of inhibitor concentration, as illustrated for complex **20** and wild-type enzyme (inset in Figure 5A), showed hyperbolic curves allowing determination of k_i as 0.102 min^{-1} and second-order rate constants k_i/K_I as 10.8 M^{-1} s^{-1}. The most potent inhibitor of the human enzyme as judged from IC_{50} values, complex **20**, was selected as a model in our inactivation studies with mutant enzymes. The DmTrxR Cys→Sec mutant enzyme (SCUS) is alkylated by cisPt complex **20** with a higher efficiency than the wild-type enzyme (SCCS), in agreement with a higher bimolecular rate constant k_i/K_I (17.9 versus 10.8 M^{-1} s^{-1}) (Figure 5B). This result confirmed that the C-terminal active site of DmTrxR is the locus of alkylation by cis-Pt derivatives. The DmTrxR mutant in which the surrounding serine residues were replaced by glycine exhibited k_i value which is 7.8-fold lower than that of the wild-type serine-containing enzyme, i.e., 0.102 min^{-1} (SCCS) and 0.013 min^{-1} (GCCG), respectively. The resulting $t_{1/2}$ values were determined as 6.8 and 53.3 min, respectively. This finding supports the influence of the serine residues 488 and 491 on the reactivity state of the terminal cysteines in the wt enzyme, as suggested earlier.[31] The bimolecular rate constant k_i/K_I for the Dm GCCG mutant of 8.5 M^{-1} s^{-1} could only be calculated from time-dependent inactivation experiment performed with inhibitor in DMSO solution instead of DMF. The influence of DMSO was directly observed on the k_i value which was evaluated as 5-fold higher than in the presence of DMF under same conditions, i.e., 0.05 min^{-1} versus 0.013 min^{-1}. It is well-known that exchange of one chloride ligand by a DMSO molecule induces a positive charge at the metal atom, thus increasing the reactivity toward thiol attack and consequently the rate of the inactivation process. Such DMSO effects were previously reported to enhance both the cytotoxicity and inhibition of DNA synthesis.[27]

Cytotoxicity. A panel of human and mouse tumor lines was tested for cytotoxic effects of compounds **13a**, **13b**, **13c**, and **20** in dose response experiments (Table 2). For comparison, cisPt was tested on the same cell lines. Tumor cell lines were selected upon their sensitivity to cisPt (Calu-6, highly sensitive; SK-MEL-25, moderately sensitive; and MCF-7, almost resistant). A 35-fold higher concentration of cisPt was needed to kill MCF-7 cells (IC_{50} = 63.7 μM) as compared to Calu-6 (IC_{50} = 1.8 μM). In contrast, the concentration of **13a**, **13b**, **13c** and **20** required to kill MCF-7 cells had only to be doubled (IC_{50} ranging from 46.3 to 55.9 μM) in comparison to Calu-6 (IC_{50} ranging from 25.0 to 29.1 μM). Furthermore, the absolute concentration of each of the four platinum complexes required to kill MCF-7 was lower than for cisPt itself, indicating a higher potency to inhibit the hTrxR/Trx-dependent growth of the most resistant cell lines.

Table 2. Antiproliferative Effects of the Platinum Complexes **13a**−**c** and **20** on Various Cancer Cell Lines

	IC_{50} (μM)[a]				
cell line	**13a**	**13b**	**13c**	**20**	cisPt
MCF-7	55.9 (0.9)	52.0 (0.8)	46.3 (0.7)	53.1 (0.8)	63.7 (1)
SK-MEL-25	15.9 (3.2)	15.0 (3.0)	14.0 (2.8)	15.1 (3.0)	5.0 (1)
Calu-6	25.0 (13.9)	29.1 (16.1)	26.5 (14.7)	27.6 (15.3)	1.8 (1)

[a] The ratio $IC_{50\ \mathbf{13a-c-20}}/IC_{50\ cisPt}$ for each derivative is given in parentheses.

DNA Interaction Studies. The four tested substances reacted strongly with DNA at a concentration of 1 mM (Figure 6). No DNA was visible in the gel any longer. This is probably due to extended cross linking which prevents the DNA from entering the gel. At a drug concentration of 0.1 mM, a partial cross linking was obtained. The amount of DNA and the mobility of the individual bands were found to be reduced. At 0.01 mM of the tested compound, DNA samples were indistinguishable from control DNA. A similar pattern was obtained with cisPt. Partial interaction with DNA was observed at 0.1 mM and no reaction at 0.01 and 0.001 mM.

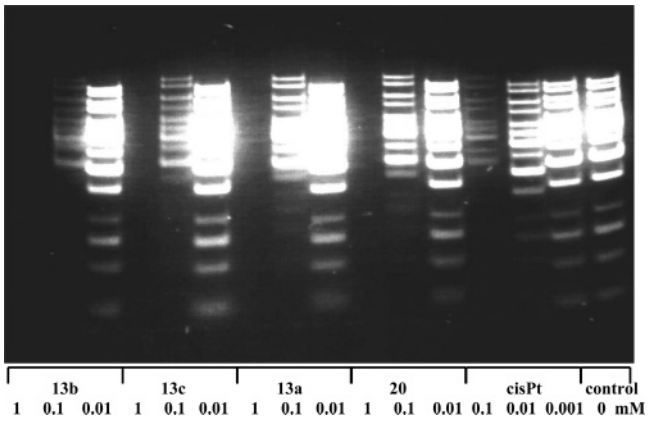

Figure 6. Effects of Complexes **13a**−**c**, **20** and cisPt on electrophoretic mobility of DNA. A mix of DNA fragments was incubated with platinum compounds at a concentration of 1, 0.1, 0.01, or 0.001 mM, as indicated. DNA samples were separated by electrophoresis on an agarose gel, followed by staining with ethidium bromide. The gel was photographed under UV light. Binding of platinum compounds to DNA is visualized by shift of electrophoretic mobility in agarose.

Discussion

The common cytostatic agent cisPt is clinically used for the treatment of many malignancies. However, many initially sensitive tumors develop resistances against this drug after the first cycles of treatment, requiring an increase in cisPt dosage to maintain antitumoral activity. Increase in dosage is however limited by the severe side effects of the drug, particularly myelo-, neuro- and nephrotoxicity. Therefore, many efforts in designing novel Pt-based drugs have been made to overcome resistance, to increase the solubility in water and to cure a broader range of cancers. Enzyme inhibition may contribute to undesirable and toxic side effects as consequences of chemotherapy or may reinforce the antitumoral effects by interaction with additive or synergistic targets for cancer therapy. Platinum complexes are often very reactive toward the cysteine residue of GSH, which detoxifies these compounds by a rapid binding mechanism.[42] Indeed, cisPt itself illustrates the positive combined effects of DNA binding and enzyme inhibition, in particular in hTrxR inhibition.[11] Formation of the GS−Pt adduct, which is a major route for elimination of cisPt, is also a toxic event for the cancer cells after irreversible inactivation of hTrxR, more potent than with the parent cisPt itself, by disturbing the redox equilibrium.[33] The aim in our studies was the design of cisPt derivatives by attaching a motif known to recognize hTrxR to the ethanediamine chain in order to increase the binding to the target according to a biligand approach. Irreversible inactivation was desired to optimize the cytotoxicity in cancer cells producing high levels of GSH and Trx.[42−44]

Screening and Chemistry. The screening of a 12 000-members library of chemicals resulted in only one inhibitor of human TrxR, the lead 5-nitro-2-furancarbohydrazide **8**, with inhibitory potencies higher than those of known inhibitors selected as references. Previous studies have demonstrated that nitrofurans are potent inhibitors of the disulfide reductase family, including glutathione reductase[29] and trypanothione reductase[34] which do not possess a second redox center in the C-terminal part of the protein. Nitroaromatic compounds including nitrofurans, nitrobenzenes and nitroimidazoles are known to exert their cytotoxic effects through their nitroreductase activities. The targets belong to the flavin-dependent oxidoreductase family that catalyzes one- or two-electron reducing reactions. Nitrofurans act as redox-cyclers; they were also described as subversive substrates or turncoat inhibitors of these flavoenzymes. In the presence of yeast GR, numerous nitrofurans showed an uncompetitive inhibition type with respect to both NADPH and GSSG.[29] Among the TrxR family, only the small TrxR from *Arabidopsis thaliana* was reported to reduce nitrofurans so far.[30] The site where reduction of nitrofurans takes place in the flavoprotein structure is not yet identified. New compounds were designed from the lead nitrofuran derivative **8** as bitopic inhibitors, a reversible nitrofuran attached to a cisPt moiety to allow the irreversible binding of the C-terminal Sec in hTrxR, both to optimize TrxR inhibition and to overcome cisPt resistance. It is well documented that the attachment of small untethered molecules only binding in the micromolar to millimolar range to proximal subsites of target proteins leads to bitopic molecules with submicromolar affinity.[45]

While nitroaromatic derivatives are not the preferred candidates for drug development, the very low mutagenic properties reported for 5-nitro-2-furohydrazide derivatives among three structure-related series of 5-nitrofuran derivatives prompted us to investigate the chemistry of the lead 5-nitro-2-furancarbohydrazide **8** to develop hTrxR inhibitors as potential anticancer drugs.[46]

Interpretation of Steady-State Kinetics with Nitrofuran Carbohydrazide 8 and the Four CisPt Complexes. The uncompetitive kinetics on wild-type hTrxR when DTNB is varied showed that prior DTNB binding to the reduced enzyme promotes association of the lead nitrofuran **8** to another site. The dissociation constant K_i for formation of the reversible complex was 16 μM, underlining the significant affinity of the lead inhibitor for a yet unidentified binding site of hTrxR. The competitive kinetics observed for DTNB reduction catalyzed by hTrxRΔ-16 implied that DTNB binding to the reduced truncated enzyme decreases affinity for the lead compound **8** at the N-terminal binding site. Thus, these studies are consistent in suggesting that the binding of the lead compound **8** is promoted by prior association of the substrate to the C-terminal part of reduced wt-hTrxR. Furthermore, DTNB competes with the lead compound **8**, both are small electron acceptors, for the N-terminal binding site of the truncated enzyme.

The last result was also confirmed by the time-dependent inactivation experiments. After attachment of the cisPt moiety to the lead compound **8**, the resulting four cisPt complexes **13a**−**c** and **20** were found to inactivate the authentic wt-hTrxR with K_i in the nanomolar range (84 nM to 275 nM). This is the successful result of the biligand strategy to design potent inhibitors of large TrxRs.

Time-Dependent Inactivation of Large TrxRs by the Four CisPt Complexes. IC_{50} values were measured from 10 min preincubation assays with mutant TrxRs in addition to the wild-type TrxR. In these assays, the submicromolar IC_{50} values determined in wt-hTrxR assays and the IC_{50} values determined in the micromolar range confirmed the selenocysteine as the main target of the cisPt complexes. The lowest IC_{50} values (21−38 μM) obtained in Trx reduction assays versus the high IC_{50} values (130−265 μM) obtained in DTNB reduction assays with the Sec498Cys mutant are in agreement with competition at the N-terminal active site between DTNB, but not Trx, and the four cisPt complexes.

In the present study, we observed a potent and irreversible inhibition of authentic human TrxR by the four cisPt complexes derived from 5-nitro-2-furancarbohydrazide **8**. Inactivation increased with time of preincubation in enzyme−NADPH−inhibitor solutions and was not reversible after dialysis. Evaluation yielded a rate constant k_i of 0.96 min^{-1}, describing the conversion of the preformed reversible hTrxR·inhibitor **20** complex to an irreversibly inhibited enzyme (dissociation constant value $K_{I,SC}$ of 30 nM for the *cis*-diamminedichloroplatinum (II) moiety of complex **20** at the C-terminal redox center). With regard to the C-terminal binding site and the mechanism of inhibition, the selenocysteine is predicted to be the target of alkylation by the four cisPt complexes since its replacement by a cysteine or its absence in the truncated enzyme led to a drastic decrease in inactivation. Finally, the determined inhibition parameters evidenced the improved potency of the inactivation process by the bitopic inhibitor **20** and its analogues compared to cisPt itself.

Cooperative Effect Induced by Nitrofuran Carbohydrazide 8 and the Four cisPt Complexes. A clear induced cooperative effect in the course of hTrxR inactivation by inhibitors **13a**−**c** and **20** could be observed for the first time. This observation is not really surprising since a 3D-structure model of the mammalian TrxR-Trx complex was suggested to explain the electron transfer from NADPH to the disulfide of the substrate by involving the motion of the C-terminal tail without large conformational changes. So far the only three-dimensional structure of a large TrxR is that of rat TrxR SeCys498Cys mutant·$NADP^+$ complex determined to 3.0 Å resolution by X-ray crystallography.[17] The overall structure is similar to that of glutathione reductase, including conserved amino acid residues binding the cofactors FAD and NADPH. The structure of the reduced enzyme shows a surface-exposed conformation of the C terminal tail. By contrast, the oxidized enzyme is proposed to have its last terminal residues buried at the active site since they are not accessible to the protease[13,14] or to chemical modification.[15] The absence of drastic steric clashes in the conformational changes of the very C-terminal tail in the step $EH_2 \rightarrow EH_4$ might explain why cooperative effects were not observed in kinetics with both NADPH and Trx.

Specificity of hTrxR inhibition. To estimate the specificity of the inhibition, the cisplatinum complexes were also tested on the structurally and mechanistically closely related, but selenium-free hGR. While all residues directly interacting with the substrate glutathione disulfide (GSSG) in GR are conserved in hTrxR, the failure of GSSG to act as substrate for TrxR strongly suggests that these residues are not exposed to allow its binding. In our studies, human GR was found far less susceptible (by a factor of 5 to 16) to inhibition than hTrxR. These data again indicate that the cisplatinum complexes bind covalently and specifically to the exposed selenocysteine residue. The inhibition of hGR might be related to nitrofuran recognition at the very conserved N-terminal active site.

Structure−Activity Relationships and Cytotoxicities. The structure−activity relationships of this first generation of cisPt complexes showed that little chemical modifications were made to observe a broad spectrum of inhibitory potencies and cytotoxicities. An apparently conflicting finding was that our four cisPt complexes induced a potent irreversible inhibition of the isolated hTrxR whereas their cytotoxic effects on three different tumor cell lines were only moderate, even though they are more effective than cisPt itself on the most resistant cell line MCF-7. Several explanations may account for these observations. First, the primary target of cisPt is DNA. After covalent linkage of cisPt by the nitrofuran via a spacer, the capability of the newly synthesized cisPt derivatives to bind DNA was shown not to be altered. Interaction with DNA was observed at a similar effective concentration as with cisPt. In contrast, the cytotoxic effect of cisPt was significantly more pronounced in sensitive cell lines. Therefore, the differences in antitumoral activity cannot be attributed to reactivity with DNA. In intact cells DNA is packed with a huge amount of proteins. Therefore, the accessibility for platinum compounds may be hindered. The sterically less demanding cisPt may reach DNA in the nucleus much easier. In addition, transport of platinum compounds through the plasma membrane is a sensitive process which might be affected by the tested compounds. Alternatively, either the four cisPt complexes possess amide bonds that could be cleaved in tumoral cells, or the structure of the four complexes is not appropriate for high cell permeability, or adducts with glutathione are rapidly extruded out off the cells. It might furthermore be possible that the alkylated hTrxR is reactivated by an unknown intracellular mechanism. Nevertheless, the higher cytotoxicity of the four cisPt complexes versus cisPt against the breast cancer MCF-7 strain supports that TrxR indeed contributes to cell growth, drug sensitivity, and DNA repair in tumor cells, particularly in resistant cell lines.

Conclusion

We have demonstrated that the four cisPt complexes based on the lead nitrofuran carbohydrazide **8** are potent and specific inhibitors of large TrxRs. The four cisPt complexes revealed to be valuable tools to study

the mechanism of these multisite enzymes. These results encouraged us to explore new linkages and to vary spacer lengths between the cisPt moiety and the TrxR inhibitors for designing a second generation of potential anticancer drugs. TrxR may be of importance for the development of new platinum complexes which circumvent resistance to cisplatinum. The additional low but significant inhibition of human GR might be a positive property to exploit for the design of potential anticancer multitarget drugs that aim at overcoming drug resistance. Work is now in progress to optimize hTrxR binding while maintaining DNA alkylation properties by preparing new bidrugs based on other lead structures that act act as irreversible hTrxR inhibitors with more appropriate pharmacokinetic properties.

Experimental Section

Abbreviations. AA, amino acid, DMSO, dimethyl sulfoxide; DTNB, 5,5′-dithiobis(2-nitrobenzoic acid); DTNBA, 5,5′-dithiobis{*N*-[3-(dimethylamino)propyl]-2-nitrobenzamide}; GSH, reduced glutathione; GSSG, glutathione disulfide; GR, glutathione reductase (EC 1.8.1.7.); hGR, human glutathione reductase; P_{HPLC}, purity determined by HPLC; PyBrop, bromotris-pyrrolidino-phosphonium hexafluorophosphate; TLC, thick-layer chromatography; Trx, thioredoxin; $Trx(S)_2$, oxidized thioredoxin; $Trx(SH)_2$, reduced thioredoxin; TrxR, thioredoxin reductase (EC 1.8.1.9.); hTrxR, human thioredoxin reductase; TOFMS, time-of-flight mass spectrometry; ICPMS, induced coupled plasma mass spectrometry.

Materials. Human cytosolic thioredoxin reductase (hTrxR) was purified from placenta as described by Gromer et al.[19] Recombinant mutant thioredoxin reductase (hTrxRSec498Cys) and hTrxRΔ-16 were used for comparative and mechanistic studies and prepared by standard techniques (Urig et al., unpublished data). In brief, the hTrxR-1 gene was amplified by PCR from a human cDNA library. Site-directed mutagenesis (QuickChange, Stratagene) was used for the replacement of selenocysteine by cysteine (hTrxRSec498Cys), and C-terminal truncation (hTrxRΔ-16) was done using standard PCR techniques. The products were cloned into the pQE30 expression vector (Qiagen) and propagated in *E. coli* M15 cells. Protein was expressed and subsequently purified over a Ni−NTA column (Novagene) via its N-terminal hexahistidyl-tag (Urig et al., unpublished data). Recombinant *D. melanogaster* thioredoxin reductase and two mutants, referred to their C-terminal tetrapeptide sequence (−SCCS = wild-type, −SCUS, and GCCG) were prepared as described earlier.[31] Recombinant human glutathione reductase (hGR) was produced and isolated according to Nordhoff et al.[47] Recombinant *E. coli* thioredoxin (EcTrx) was kindly provided by Prof. Charles Williams, Ann Arbor, MI. Recombinant human mutant thioredoxin (hTrxC72S) and *D. melanogaster* thioredoxin-2 (DmTrx) were produced and purified as previously described[21,48] and allowed to study the inhibitory effects with the respective physiological substrate. All enzymes used were pure as judged by silver stained SDS−PAGE. Flavoenzyme concentrations were determined spectrophotometrically at 463 nm using an ϵ value of 11.3 $mM^{-1}\,cm^{-1}$. In the case of DmTrxR−SCUS, atomic absorbance spectroscopy was applied as FAD-containing, but prematurely terminated protein prevents a reliable spectrophotometric determination.[3,12,47] Thioredoxin concentrations were measured enzymatically by end point determination at 340 nm. Two different assays were applied to determine thioredoxin reductase activity, the DTNB-reduction assay, where 1 unit of TrxR activity is defined as the NADPH-dependent production of 2 μmol 2-nitro-5-thiobenzoate per min ($\epsilon_{412\ nm}$ 13.6 $mM^{-1}\,cm^{-1}$), and the thioredoxin reduction assay where 1 unit of TrxR activity is defined as the consumption of 1 μmol NADPH per min ($\epsilon_{340\ nm} = 6.22\ mM^{-1}\,cm^{-1}$). Similarly, one unit of GR activity is defined as the consumption of 1 μmol NADPH per min ($\epsilon_{340\ nm} = 6.22\ mM^{-1}\,cm^{-1}$). Specific activities were essentially identical as reported earlier, i.e. 10−27 U/mg for wild-type hTrxR in the DTNB-assay,[19,49] and of 170 U/mg for hGR in the GSSG-assay,[47] respectively. The newly described hTrxRΔ-16 mutant's activity was below the detection limit in the thioredoxin reduction assay and reached 1.4% (0.41 U/mg) of the authentic enzyme activity in the DTNB-reduction assay, a value similar to data observed for the rat TrxRSec498Cys[41] and the respective human enzyme of this work (0.35 U/mg). All reagents used were of the highest commercially available purity and obtained from Alfa, Boehringer, Serva, and Sigma, Germany.

Inhibitor Screening with Human Thioredoxin Reductase. For preliminary inhibitor studies and high-throughput inhibitor screening in microtiter plates, DTNBA disulfide[28] was used as artificial substrate of hTrxR according to the reported procedures for hTrxR inhibition studies.[50] The formation of 5-thio-2-nitrobenzamide liberated from DTNBA reduction was followed by measuring the absorbance at 416 nm and plotted as a function of time in both the absence and presence of 50 μM inhibitor. The DTNBA disulfide concentration of the 5 mM stock solution in DMSO was adjusted spectrophotometrically by using $\epsilon_{327\ nm}$ of 15,600 ± 80 $mM^{-1}\,cm^{-1}$. All reactions with hTrxR were performed in 100 mM sodium phosphate, 2 mM EDTA, pH 7.0. The standard assay mixture for HTS contained 500 μM NADPH, 200 μM DTNBA, and 25 μM inhibitor and the reaction was started with native enzyme (8.0×10^{-4} units in 100 μL total volume). The commercially available TrxR inhibitor 2,6-dichloroindophenol was used as reference inhibitor. Confirmation of the positive hits and evaluation of further intermediates of synthetic procedures was performed spectrophotometrically by measuring IC_{50} values in duplicate in the presence of 50 μM DTNBA, increasing inhibitor concentrations (5−50 μM) and 1% DMSO as final concentration. The reaction was started by adding native enzyme (7.2×10^{-3} units in 500 μL total volume).

TrxR-Catalyzed Nitrofuran Reductase Activity. The ability of TrxR to reduce the nitrofuran lead compound was assayed at 25 °C by monitoring the oxidation of NADPH at 340 nm ($\epsilon_{340} = 6.22\ mM^{-1}\,cm^{-1}$). The assays, in a total volume of 1 mL, contained TrxR-buffer (100 mM potassium phosphate, 2 mM EDTA, pH 7.4) and 0.386 units TrxR. The nitrofuran was dissolved in DMSO, and the NADPH-oxidase activity was measured at 10 different concentrations (10−400 μM) in the presence of 1% DMSO. For the determination of K_m and V_{max} values, the steady-state rates were graphically fitted by using nonlinear regression analysis software (Kaleidagraph) to the Michaelis−Menten equation, and the turnover number k_{cat} and the catalytic efficiency k_{cat}/K_m were calculated. The initial rate of intrinsic NADPH oxidase activity of *P. falciparum* TrxR was not subtracted from the rates measured in the presence of the nitrofuran, since it proved negligible in comparison to the TrxR-catalyzed nitrofuran reductase activity.

Inhibition of Wild-Type and of Truncated Human TrxR by Lead Compound 8 in the Steady-State. The DTNB reducing activity of wild-type and of truncated human TrxR was assayed by monitoring the formation of thionitrobenzoate, TNB^-, at 412 nm ($\epsilon_{412\ nm} = 13.6\ mM^{-1}\,cm^{-1}$) due to oxidation of NADPH. The assay mixtures, in a total volume of 0.5 mL, contained TrxR-buffer, and 1.8 milliunits wild-type TrxR and 3.4 milliunits of truncated human hTrxRΔ-16, respectively. For determination of K_m and V_{max}, the data were fitted to the Michaelis−Menten equation using the computerized least-squares regression program Kaleidagraph. Evaluation of inhibition type and inhibition constants for inhibitor **8** was done in duplicate experiments using 200 μM NADPH. Wild-type TrxR activity was measured at different concentrations of inhibitor **8** (0−40 μM) in the presence of varying concentrations of DTNB (11−435 μM). Truncated human hTrxRΔ-16 activity was measured at different concentrations of inhibitor **8** (0−250 μM) in the presence of varying concentrations of DTNB (0.6−6.0 mM). Inhibition was measured as a function of DTNB concentration, and the data were fitted to the appropriate equation by using nonlinear regression analysis software (Kaleidagraph).

Time-Dependent Inactivation of Human Thioredoxin Reductase by the Four cisPt Complexes. Relative IC_{50} Values from Time-Dependent Inactivation of Wild-Type and Mutant Human TrxRs. Apart from the inhibitor screening studies all further inhibition studies were performed in a total volume of 500 μL at 25 °C in 100 mM potassium phosphate, 2 mM EDTA, pH 7.4. Either the DTNB assay (3 mM DTNB and 200 μM NADPH; $\epsilon_{412\ nm} = 13.6\ mM^{-1}\ cm^{-1}$ for the formation of one TNB anion) or the Trx assay (20 μM hTrxC72S and 100 μM NADPH; $\epsilon_{340\ nm} = 6.22\ mM^{-1}\ cm^{-1}$) was used. IC_{50} values given in Table 1 were measured when hTrxR (5 nM) or hTrxRSec498Cys (100 nM) was incubated for 10 min with NADPH and varying concentrations of inhibitor (10 mM stock solution in DMF) at 25 °C. The assays were started with DTNB and hTrxC72S, respectively, and DMF was used in control assays.

Time-Dependent Inactivation of Wild-Type Human TrxR. For determining rate constants of hTrxR inactivation TrxR activity was monitored over the time by following a preincubation protocol. To a final volume of 500 μL TrxR buffer were added at 25 °C 100 μM NADPH, 0−36.6 μM inhibitor, and 1.83 μM TrxR. All reaction mixtures contained 2% DMF. At different time points 5 μL aliquots of each reaction mixture were removed, and the residual activity was measured in the standard Trx reduction assay at 25 °C.[51]

Inhibition of Human TrxR by the Four cisPt Complexes in the Steady-State. For determining type and constants of wt-hTrxR inhibition by varying concentrations of inhibitor **13a**−**c** and **20** (0−800 nM), the reactions were started following NADPH addition without preincubation. The standard DTNB reduction assay mixtures contained 200 μM NADPH, varying concentrations of DTNB (100−500 μM), 10 nM wt-hTrxR. The DTNB reduction was monitored at 412 nm, following TNB formation. The standard Trx reduction assay mixtures contained 100 μM NADPH, varying concentrations of hTrxC72S (8−100 μM), 20 nM wt-hTrxR. Initial Trx reduction rates were recorded from NADPH oxidation at 340 nm and 25 °C. To study the inhibition of hTrxRSec498Cys in the presence of 20 to 250 μM inhibitor, the standard DTNB reduction mixtures contained 100 nM mutant enzyme and varying concentrations of DTNB (100−4000 μM), while Trx reduction was monitored in assays using 1.3 μM mutant enzyme and 10 to 100 μM Trx.

Inhibition of Glutathione Reductase. The inhibition of human glutathione reductase was tested at 25 °C in 47 mM potassium phosphate, 1 mM EDTA, 200 mM KCl, pH 6.9. After preincubation of 2−10 mU/mL enzyme with 100 μM NADPH and varying inhibitor concentrations, the assay was started with 100 μM GSSG and the consumption of NADPH was monitored as the decrease in absorbance at 340 nm.[47] IC_{50} values were determined in comparison with DMF-containing controls.

Time-dependent Inactivation of *D. melanogaster* Thioredoxin Reductase. DmTrxR (2 μL of 123.9 μM enzyme solution) was incubated at 25 °C in a final volume of 50 μL of 100 mM potassium phosphate buffer pH 7.4, with 160 μM NADPH and the inhibitor at different concentrations (2% final DMF concentration was kept constant) for 60 min. Final concentrations of inhibitors **13a**−**c** and **20** in the preincubation mixture were 0−10−25−50 μM. The inactivation process was stopped by diluting a 5 μL aliquot of each incubation mixture into a UV cuvette containing buffer to measure the residual Trx reducing activity. The reaction mixture consisted of 100 mM potassium phosphate buffer pH 7.4, 2 mM EDTA, 100 μM NADPH, 1 mM GSSG, and 43.6 μM DmTrx (0.5% DMF final). The loss of *D. melanogaster* TrxR activity was determined by monitoring Trx reduction as a function of time of the preincubation mixture.[51] NADPH oxidation was monitored at 340 nm.

Cytotoxicity Assays. Calu-6 (adenocarcinoma, lung), SK-MEL 25 (melanoma), and MCF-7 (mamma carcinoma) cells were obtained from the American Type Culture Collection and were cultivated according to instructions of the supplier at 37 °C in Dulbecco's modified Eagle's medium (DMEM) in a 5% CO_2 atmosphere. Cytotoxicity was determined as described previously.[52] One mg/mL stock solutions of the platinum complexes in DMF were prepared. Cisplatin (Alfa, Karlsruhe) was dissolved in water at a concentration of 0.5 mg/mL. A maximum concentration of 50 μg/mL was applied to the cells for all compounds. Cells were grown in 96-well plates at a density of 2×10^6 cells/plate. One day later, test compounds were added in quadruplicate. Serial 1:2 dilutions were prepared directly on the plates using multichannel pipets. The resulting inhibitor concentrations were 50, 25, 12.5, 6.25, 3.1, 1.6, and 0.8 μg/mL. After incubation for 96 h, cells were fixed with 3% formaldehyde and stained with 1% crystal violet. The amount of bound crystal violet, which is linearly dependent on the number of adherent, surviving cells was determined in an Antos 2001 ELISA reader at 595 nm. In the case of MCF-7 cells, which grow inhomogeneously, the dye was eluted with 200 μL ethanol/1% acetic acid before absorption determination. IC_{50}-values were taken from dose−response curves after curve fitting.

DNA Interaction Studies. Stock solutions of tested substances in DMF (10 mM) were prepared and used within 1 h. Gene ruler 1kb DNA Ladder (MBI) was diluted with water to a final concentration of 50 μg/mL. DNA samples (50 μL each) were mixed with the tested substances to a final concentration of 1, 0.1 and 0.01 μM. cisPt was added to a concentration of 0.1, 0.01, and 0.001 mM. One sample was treated with 10% DMF as a control. Samples were incubated at room temperature for 16 h. Aliquots of 25 μL were electrophoresed into a 1.4% agarose gel (100 mM Tris/phosphate buffer) at 5 V/cm for 3 h. The gel was stained with ethidium bromide and photographed under UV light.

Acknowledgment. This work was supported by Institut Pasteur de Lille (Fellowship attributed to R.M.), by the Centre National de la Recherche Scientifique-Forschungsgemeinschaft Funds 02N40/0800 (E.D.-C, S.G., K.B.) and by the Deutsche Forschungsgemeinschaft (Be 1540/6−2 to K.B., GR 2028/1-1 to S.G.). The authors are grateful to Athel Cornish−Bowden and Maria Luz Cardenas for fruitful discussions. They also thank Anick Lemaire (CNRS France, Lille) and Elisabeth Fischer (Giessen University) for their excellent contribution in the primary screening of the 12 000 compound-based library and technical assistance, respectively. Mathieu Sauty and Julien Furrer are acknowledged for recording ICP-MS spectra (Service Eaux Environnement, Institut Pasteur de Lille, Dr. Pierre Thomas) and ^{195}Pt NMR spectra (Organisch-Chemisches Institut, Heidelberg University), respectively.

Supporting Information Available: Experimental procedures, spectrosopic data, and elemental analyses for the preparation and the characterization of compounds **1** to **20** are available free of charge via the Internet at http://pubs.acs.org.

References

(1) Wong, E.; Giandomenico, C. M. Current status of platinum-based antitumor drugs. *Chem. Rev.* **1999**, *99*, 2451−2466.
(2) Reedijk, J. Why does Cisplatin reach Guanine-n7 with competing s-donor ligands available in the cell? *Chem. Rev.* **1999**, *99*, 2499−2510.
(3) Gromer, S.; Urig, S.; Becker, K. The thioredoxin system—from science to clinic. *Med. Res. Rev.* **2004**, *24*, 40−89.
(4) Holmgren, A. Thioredoxin and glutaredoxin systems. *J. Biol. Chem.* **1989**, *264*, 13963−13966.
(5) Krnajski, Z.; Gilberger, T. W.; Walter, R. D.; Cowman, A. F.; Muller, S. Thioredoxin reductase is essential for the survival of *Plasmodium falciparum* erythrocytic stages. *J. Biol. Chem.* **2002**, *277*, 25970−25975.
(6) Missirlis, F.; Ulschmid, J. K.; Hirosawa-Takamori, M.; Gronke, S.; Schafer, U.; Becker, K.; Phillips, J. P.; Jackle, H. Mitochondrial and cytoplasmic thioredoxin reductase variants encoded by a single *Drosophila* gene are both essential for viability. *J. Biol. Chem.* **2002**, *277*, 11521−11526.

(7) Missirlis, F.; Phillips, J. P.; Jackle, H. Cooperative action of antioxidant defense systems in *Drosophila*. *Curr. Biol.* **2001**, *11*, 1272−1277.
(8) Jakupoglu, C.; Przemeck, G. K.; Schneider, M.; Moreno, S. G.; Mayr, N.; Hatzopoulos, A. K.; de Angelis, M. H.; Wurst, W.; Bornkamm, G. W.; Brielmeier, M.; Conrad, M. Cytoplasmic thioredoxin reductase is essential for embryogenesis but dispensable for cardiac development. *Mol. Cell Biol.* **2005**, *25*, 1980−1988.
(9) Conrad, M.; Jakupoglu, C.; Moreno, S. G.; Lippl, S.; Banjac, A.; Schneider, M.; Beck, H.; Hatzopoulos, A. K.; Just, U.; Sinowatz, F.; Schmahl, W.; Chien, K. R.; Wurst, W.; Bornkamm, G. W.; Brielmeier, M. Essential role for mitochondrial thioredoxin reductase in hematopoiesis, heart development, and heart function. *Mol. Cell Biol.* **2004**, *24*, 9414−9423.
(10) Anestål, K.; Arnér, E. S. Rapid induction of cell death by selenium-compromised thioredoxin reductase 1 but not by the fully active enzyme containing selenocysteine. *J. Biol. Chem.* **2003**, *278*, 15966−15972.
(11) Sasada, T.; Nakamura, H.; Ueda, S.; Sato, N.; Kitaoka, Y.; Gon, Y.; Takabayashi, A.; Spyrou, G.; Holmgren, A.; Yodoi, J. Possible involvement of thioredoxin reductase as well as thioredoxin in cellular sensitivity to cis-diamminedichloroplatinum (II). *Free Radic. Biol. Med.* **1999**, *27*, 504−514.
(12) Arscott, L. D.; Gromer, S.; Schirmer, R. H.; Becker, K.; Williams, C. H., Jr. The mechanism of thioredoxin reductase from human placenta is similar to the mechanisms of lipoamide dehydrogenase and glutathione reductase and is distinct from the mechanism of thioredoxin reductase from *Escherichia coli*. *Proc. Natl. Acad. Sci. U.S.A.* **1997**, *94*, 3621−3626.
(13) Gromer, S.; Wissing, J.; Behne, D.; Ashman, K.; Schirmer, R. H.; Flohe, L.; Becker, K. A hypothesis on the catalytic mechanism of the selenoenzyme thioredoxin reductase. *Biochem. J.* **1998**, *332* (*Pt 2*), 591−592.
(14) Zhong, L.; Arnér, E. S.; Ljung, J.; Åslund, F.; Holmgren, A. Rat and calf thioredoxin reductase are homologous to glutathione reductase with a carboxyl-terminal elongation containing a conserved catalytically active penultimate selenocysteine residue. *J. Biol. Chem.* **1998**, *273*, 8581−8591.
(15) Lee, S. R.; Bar-Noy, S.; Kwon, J.; Levine, R. L.; Stadtman, T. C.; Rhee, S. G. Mammalian thioredoxin reductase: oxidation of the C-terminal cysteine/selenocysteine active site forms a thioselenide, and replacement of selenium with sulfur markedly reduces catalytic activity. *Proc. Natl. Acad. Sci. U.S.A.* **2000**, *97*, 2521−2526.
(16) Bauer, H.; Massey, V.; Arscott, L. D.; Schirmer, R. H.; Ballou, D. P.; Williams, C. H., Jr. The mechanism of high Mr thioredoxin reductase from *Drosophila* melanogaster. *J. Biol. Chem.* **2003**, *278*, 33020−33028.
(17) Sandalova, T.; Zhong, L.; Lindqvist, Y.; Holmgren, A.; Schneider, G. Three-dimensional structure of a mammalian thioredoxin reductase: implications for mechanism and evolution of a selenocysteine-dependent enzyme. *Proc. Natl. Acad. Sci. U.S.A.* **2001**, *98*, 9533−9538.
(18) Kaim, W.; Schwederski, B. *Bioanorganische Chemie. Zur Funktion chemischer Elemente in Lebensprozessen,* 2nd ed.; Teubner Verlag: Stuttgart, 1995; p 460.
(19) Gromer, S.; Arscott, L. D.; Williams, C. H., Jr.; Schirmer, R. H.; Becker, K. Human placenta thioredoxin reductase. Isolation of the selenoenzyme, steady-state kinetics, and inhibition by therapeutic gold compounds. *J. Biol. Chem.* **1998**, *273*, 20096−20101.
(20) Becker, K.; Herold-Mende, C.; Park, J. J.; Lowe, G.; Schirmer, R. H. Human thioredoxin reductase is efficiently inhibited by (2,2′:6′,2″-terpyridine)platinum(II) complexes. Possible implications for a novel antitumor strategy. *J. Med. Chem.* **2001**, *44*, 2784−2792.
(21) Irmler, A.; Bechthold, A.; Davioud-Charvet, E.; Hofmann, V.; Réau, R.; Gromer, S.; Schirmer, R. H.; Becker, K. Disulfide Reductases − Current Developments. *Flavins and Flavoproteins 2002*; Agency for Scientific Publications: Berlin, 2002; pp 803−815.
(22) Jencks, W. P. On the attribution and additivity of binding energies. *Proc. Natl. Acad. Sci. U.S.A.* **1981**, *78*, 4046−4050.
(23) Pasini, A. A doxorubicin-Pt(II) complex with antitumor activity. Synthesis, characterization and reactions with guanosine and DNA. *Gazz. Chim. Ital.* **1987**, *117*, 763−768.
(24) Palmer, B. D.; Lee, H. H.; Johnson, P.; Baguley, B. C.; Wickham, G.; Wakelin, L. P.; McFadyen, W. D.; Denny, W. A. DNA-directed alkylating agents. 2. Synthesis and biological activity of platinum complexes linked to 9-anilinoacridine. *J. Med. Chem.* **1990**, *33*, 3008−3014.
(25) Gibson, D.; Gean, K. F.; Ben-Shoshan, R.; Ramu, A.; Ringel, I.; Katzhendler, J. Preparation, characterization, and anticancer activity of a series of cis-PtCl2 complexes linked to anthraquinone intercalators. *J. Med. Chem.* **1991**, *34*, 414−420.
(26) Perez, J. M.; Lopez-Solera, I.; Montero, E. I.; Brana, M. F.; Alonso, C.; Robinson, S. P.; Navarro-Ranninger, C. Combined effect of platination and intercalation upon DNA binding of novel cytotoxic Pt-bis(naphthalimide) complexes. *J. Med. Chem.* **1999**, *42*, 5482−5486.
(27) von Nussbaum, F.; Miller, B.; Wild, S.; Hilger, C. S.; Schumann, S.; Zorbas, H.; Beck, W.; Steglich, W. Synthesis of 1-(2-aminophenyl)isoquinolines and the biological activity of their cis-dichloro platinum(II) complexes. *J. Med. Chem.* **1999**, *42*, 3478−3485.
(28) Davioud-Charvet, E.; Becker, K.; Landry, V.; Gromer, S.; Loge, C.; Sergheraert, C. Synthesis of 5,5′-dithiobis(2-nitrobenzamides) as alternative substrates for trypanothione reductase and thioredoxin reductase: a microtiter colorimetric assay for inhibitor screening. *Anal. Biochem.* **1999**, *268*, 1−8.
(29) Cenas, N. K.; Bironaite, D. A.; Kulys, J. J.; Sikhova, N. M. Interaction of nitrofurans with glutathione reductase. *Biochim. Biophys. Acta* **1991**, *1073*, 195−199.
(30) Miskiniene, V.; Sarlauskas, J.; Jacquot, J. P.; Cenas, N. Nitroreductase reactions of *Arabidopsis thaliana* thioredoxin reductase. *Biochim. Biophys. Acta* **1998**, *1366*, 275−283.
(31) Gromer, S.; Johansson, L.; Bauer, H.; Arscott, L. D.; Rauch, S.; Ballou, D. P.; Williams, C. H., Jr.; Schirmer, R. H.; Arnér, E. S. Active sites of thioredoxin reductases: why selenoproteins? *Proc. Natl. Acad. Sci. U.S.A.* **2003**, *100*, 12618−12623.
(32) Mau, B. L.; Powis, G. Mechanism-based inhibition of thioredoxin reductase by antitumor quinoid compounds. *Biochem. Pharmacol.* **1992**, *43*, 1613−1620.
(33) Arnér, E. S.; Nakamura, H.; Sasada, T.; Yodoi, J.; Holmgren, A.; Spyrou, G. Analysis of the inhibition of mammalian thioredoxin, thioredoxin reductase, and glutaredoxin by cis-diamminedichloroplatinum (II) and its major metabolite, the glutathione-platinum complex. *Free Radic. Biol. Med.* **2001**, *31*, 1170−1178.
(34) Blumenstiel, K.; Schoneck, R.; Yardley, V.; Croft, S. L.; Krauth-Siegel, R. L. Nitrofuran drugs as common subversive substrates of *Trypanosoma cruzi* lipoamide dehydrogenase and trypanothione reductase. *Biochem. Pharmacol.* **1999**, *58*, 1791−1799.
(35) Gilberger, T. W.; Bergmann, B.; Walter, R. D.; Muller, S. The role of the C-terminus for catalysis of the large thioredoxin reductase from *Plasmodium falciparum*. *FEBS Lett.* **1998**, *425*, 407−410.
(36) Muller, D.; Zeltser, I.; Bitan, G.; Gilon, C. Building units for N-backbone cyclic peptides. 3. Synthesis of protected N(alpha)−(omega-aminoalkyl)amino acids and N(alpha)−(omega-carboxyalkyl)amino acids. *J. Org. Chem.* **1997**, *62*, 411−416.
(37) Thomas, P.; Finnie, J. K.; Williams, J. G. Feasibility of identification and monitoring of arsenic species in soil and sediment samples by coupled HPLC− inductively coupled plasma mass spectrometry. *J. Anal. At. Spectrom.* **1997**, *12*, 1367−1372.
(38) Arnér, E. S.; Bjornstedt, M.; Holmgren, A. 1-Chloro-2,4-dinitrobenzene is an irreversible inhibitor of human thioredoxin reductase. Loss of thioredoxin disulfide reductase activity is accompanied by a large increase in NADPH oxidase activity. *J. Biol. Chem.* **1995**, *270*, 3479−3482.
(39) Kitz, R.; Wilson, I. B. Esters of methanesulfonic acid as irreversible inhibitors of acetylcholinesterase. *J. Biol. Chem.* **1962**, *237*, 3245−3249.
(40) Kuo, D. J.; Jordan, F. Active site directed irreversible inactivation of brewers' yeast pyruvate decarboxylase by the conjugated substrate analogue (E)-4-(4-chlorophenyl)-2-oxo-3-butenoic acid: development of a suicide substrate. *Biochemistry* **1983**, *22*, 3735−3740.
(41) Zhong, L.; Holmgren, A. Essential role of selenium in the catalytic activities of mammalian thioredoxin reductase revealed by characterization of recombinant enzymes with selenocysteine mutations. *J. Biol. Chem.* **2000**, *275*, 18121−18128.
(42) Jansen, B. A.; Brouwer, J.; Reedijk, J. Glutathione induces cellular resistance against cationic dinuclear platinum anticancer drugs. *J. Inorg. Biochem.* **2002**, *89*, 197−202.
(43) Kearns, P. R.; Hall, A. G. Glutathione and the response of malignant cells to chemotherapy. *Drug Discovery Today* **1998**, *3*, 113−121.
(44) Baker, A.; Payne, C. M.; Briehl, M. M.; Powis, G. Thioredoxin, a gene found overexpressed in human cancer, inhibits apoptosis in vitro and in vivo. *Cancer Res.* **1997**, *57*, 5162−5167.
(45) Hajduk, P. J.; Meadows, R. P.; Fesik, S. W. Discovering high-affinity ligands for proteins. *Science* **1997**, *278*, 497−499.
(46) Kato, Y.; Inouye, T.; Jyosui, S.; Kakimoto, K.; Iyehara-Ogawa, H.; Tsuruta, S. Structure-dependent variation in the mutagenic, prophage-inducing and antibacterial activities of 5-nitro-2-furamide derivatives. *Mutat. Res.* **1984**, *140*, 169−174.
(47) Nordhoff, A.; Bucheler, U. S.; Werner, D.; Schirmer, R. H. Folding of the four domains and dimerization are impaired by the Gly446→Glu exchange in human glutathione reductase. Implications for the design of antiparasitic drugs. *Biochemistry* **1993**, *32*, 4060−4066.

(48) Bauer, H.; Kanzok, S. M.; Schirmer, R. H. Thioredoxin-2 but not thioredoxin-1 is a substrate of thioredoxin peroxidase-1 from *Drosophila melanogaster*: isolation and characterization of a second thioredoxin in *D. Melanogaster* and evidence for distinct biological functions of Trx-1 and Trx-2. *J. Biol. Chem.* **2002**, *277*, 17457−17463.
(49) Holmgren, A.; Bjornstedt, M. Thioredoxin and thioredoxin reductase. *Methods Enzymol.* **1995**, *252*, 199−208.
(50) Salmon-Chemin, L.; Buisine, E.; Yardley, V.; Kohler, S.; Debreu, M. A.; Landry, V.; Sergheraert, C.; Croft, S. L.; Krauth-Siegel, R. L.; Davioud-Charvet, E. 2- and 3-substituted 1,4-naphthoquinone derivatives as subversive substrates of trypanothione reductase and lipoamide dehydrogenase from *Trypanosoma cruzi*: synthesis and correlation between redox cycling activities and in vitro cytotoxicity. *J. Med. Chem.* **2001**, *44*, 548−565.
(51) Gromer, S.; Merkle, H.; Schirmer, R. H.; Becker, K. Human placenta thioredoxin reductase: preparation and inhibitor studies. *Methods Enzymol.* **2002**, *347*, 382−394.
(52) Amtmann, E.; Zoller, M.; Wesch, H.; Schilling, G. Antitumoral activity of a sulphur-containing platinum complex with an acidic pH optimum. *Cancer Chemother. Pharmacol.* **2001**, *47*, 461−466.
(53) Zhong, L.; Arnér, E. S.; Holmgren, A. Structure and mechanism of mammalian thioredoxin reductase: the active site is a redox-active selenolthiol/selenenylsulfide formed from the conserved cysteine-selenocysteine sequence. *Proc. Natl. Acad. Sci. U.S.A.* **2000**, *97*, 5854−5859.

JM050256L